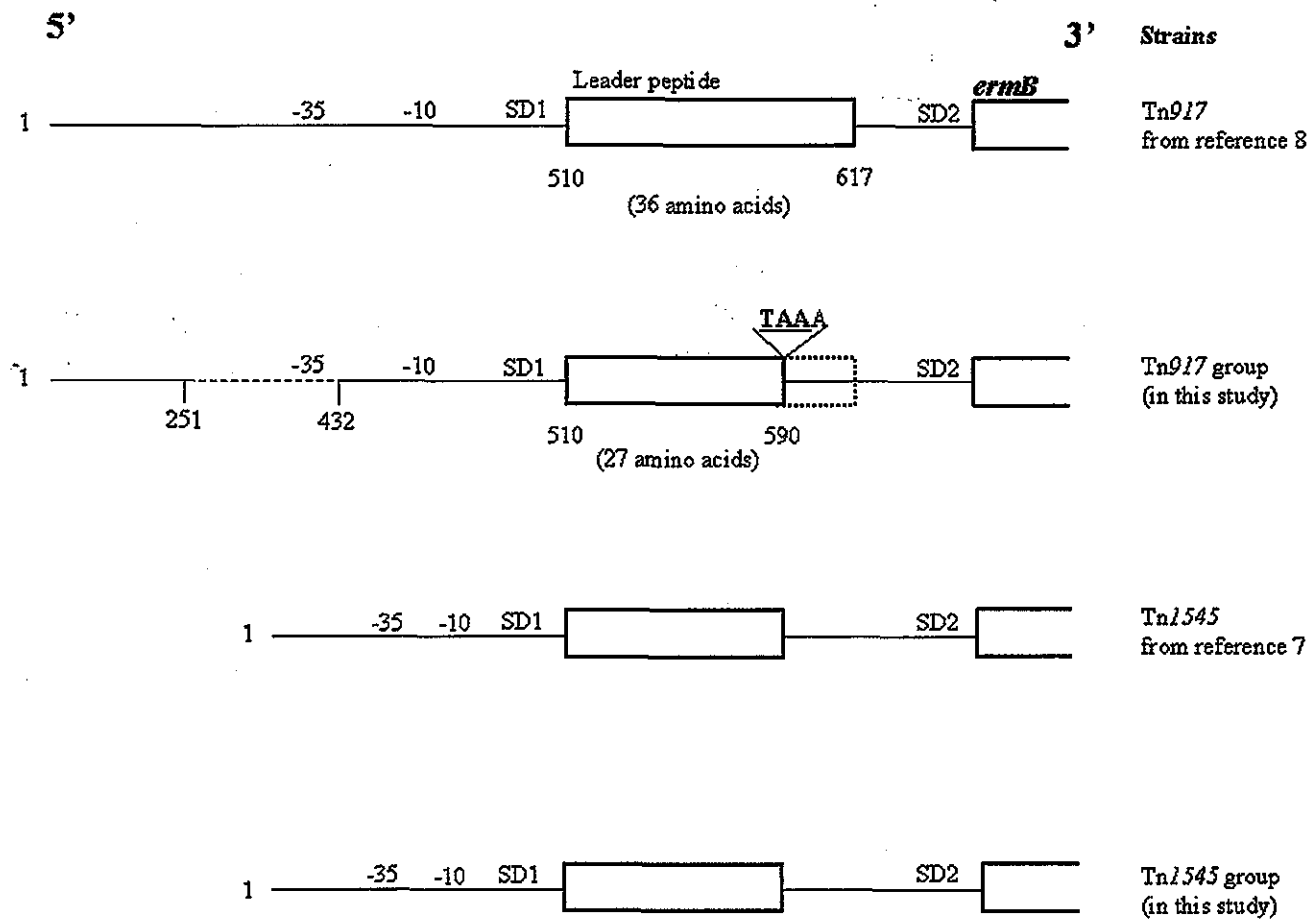

FIG. 1. Schematic representation of the reported regulatory region of the *ermB* gene on Tn*917* or Tn*1545*, and the regions found in macrolide-resistant *S. pneumoniae* in this study. SD1 and SD2, ribosome-binding sites for the leader peptide and *ermB* gene, respectively; −10 and −35, putative promoter regions according to references 7 and 8. Deletions are indicated by dashes.

TTCTGGTACTAAAAGTGG-3′ (18). Primers 5′-ATCTGACGGTGACATCT CTC-3′ and 5′-GGTTGAGTACCTTTTCATTCGTTAA-3′ for Tn*917* (17), and primers 5′-CTTAGAAGCAAACTTAAGAGTGTGT-3′ and 5′-GGTTGAGTA CCTTTTCATTCGTTAA-3 for Tn*1545* (22), were designed to amplify a fragment including the regulatory region and 48 bp of the 5′ end of *ermB*. PCR was carried out by 35 cycles of amplification consisting of 1 min of denaturation at 94°C, 1 min of annealing at 52°C, and 1 min of elongation at 72°C, followed by heating at 72°C for 7 min. PCR products were analyzed by using a DNA sequencing kit (ABI PRISM Big Dye Terminator cycle sequencing, FS; Perkin-Elmer Applied Biosystems, Tokyo, Japan). *S. pneumoniae* BM4200 containing Tn*1545*, kindly provided by P. Courvalin (Institut Pasteur, Paris, France) (22), and *E. faecalis* DS16 containing Tn*917* (17), kindly provided D. B. Clewell (University of Michigan, Ann Arbor, Mich.), were used as positive controls. Reaction products were precipitated with ethanol-potassium acetate, dissolved in template suppression reagent, and run on an ABI PRISM 310 sequencer. As a result, the organisms were separated into two groups: a Tn*917* group and a Tn*1545* group.

Analysis of reduction of telithromycin susceptibility by disk diffusion. The disk diffusion test was performed (9) using six strains selected from both groups based on the MICs for erythromycin and rokitamycin. Against the six strains, the MICs of erythromycin and rokitamycin were both >128 mg/liter (two strains), 4 and 8 mg/liter (two strains), and 4 and 1 mg/liter (two strains), respectively. Two milliliters of the bacterial suspension (approximately 10^8 CFU/ml) was spread over the surface of 10 ml of sensitivity test agar containing 8% SHS. After excess bacterial suspension was removed, paper disks (diameter, 8 mm; Tokyo Roshi Kaisha, Tokyo, Japan) impregnated with erythromycin (*20 μg/disk*), azithromycin (20 μg/disk), rokitamycin (20 and 100 μg/disk), or telithromycin (10 μg/disk) were placed on the surface of each agar plate. Then the plates were incubated overnight at 35°C. The presence of induced telithromycin resistance was assessed based on the shape of the zone of inhibition around the telithromycin disk (whether the so-called D-shape was observed).

Serogroup and genotyping analysis. The isolates were cultured in Mueller-Hinton broth (Eiken Chemical Co.) with 8% SHS at 35°C for 18 to 24 h; they were then harvested by centrifugation at 3,000 × *g* for 10 min. The serogroup of each strain was determined by using antisera for *S. pneumoniae* (Seiken Antisera; Denkaseiken, Tokyo, Japan). The isolates were genotyped by pulsed-field gel electrophoresis (PFGE), as reported previously (23), after strains from both groups were selected based on the serogroup and the geographical location of isolation in addition to the MIC for the macrolides.

Nucleotide sequence accession number. The nucleotide sequence data obtained in this study are available in the GenBank/EMBL nucleotide database under accession number AB111455.

RESULTS

PCR-based detection of resistance genes and DNA sequence analysis. Of the 84 isolates tested, all possessed the *ermB* gene and none had the *mefA* gene. There were 65 strains in the Tn*917* group and 19 in the Tn*1545* group. After selection of representative strains, comprising 19 strains from the Tn*917* group and all strains from the Tn*1545* group, with high (>128 mg/liter) or low (<4 mg/liter) erythromycin and rokitamycin MICs, the regulatory region and *ermB* gene were analyzed and aligned with the same region of *ermB* previously reported in Tn*917* and Tn*1545* (Fig. 1).

It was found that the sequences of the Tn*1545* group isolates all were identical to that reported for Tn*1545* (22). In the Tn*917* group, the sequences of 19 strains were identical to that

TABLE 1. In vitro activities of macrolides, clindamycin, telithromycin, and penicillin G against macrolide-resistant *S. pneumoniae* strains with different transposons

Group	MIC (mg/liter)[a] of:					
	Erythromycin	Azithromycin	Rokitamycin	Clindamycin	Telithromycin	Penicillin G
Tn1545 group (n = 19)						
Range	≤0.06–>128	0.25–>128	≤0.06–128	≤0.06–>128	≤0.06–>0.25	≤0.06–1
MIC_{50}	**4**	>128	**1**	128	≤0.06	0.25
MIC_{90}	128	>128	**2**	>128	0.13	0.5
Tn917 group (n = 65)						
Range	0.5–128	1–>128	2–>128	16–>128	≤0.06–0.25	≤0.06–1
MIC_{50}	**128**	>128	**32**	>128	≤0.06	≤0.06
MIC_{90}	>128	>128	**>128**	>128	0.25	0.5

[a] MIC_{50} and MIC_{90}, MICs at which 50 and 90% of isolates, respectively, were inhibited. Boldfaced values indicate prominent differences between the two groups.

reported for Tn*917* (17), but two mutations were found. The first mutation was insertion of a TAAA motif at T591 (T421 in our data) (14, 24). Since the TAAA motif is recognized as a stop codon, the putative leader peptide was shortened by 9 amino acids. The second mutation was the deletion of 182 bp from T251 to T432 (T81 to T262 in our data) (17). The −35 region of the putative promoter was included in this deletion. But the *ermB* gene was expressed, as evidenced by the fact that the strains with Tn*917* were resistant to macrolides and clindamycin. This finding suggests the presence of a new promoter.

Susceptibility. The MIC data for the macrolide-resistant *S. pneumoniae* strains with different transposons are displayed in Table 1. The MICs of erythromycin and rokitamycin were higher for strains from the Tn*917* group than for strains from the Tn*1545* group. In the Tn*1545* group, the MICs of erythromycin and clindamycin for two strains with the *ermB* gene were ≤0.25 mg/liter, but other strains exhibited the MLS_B phenotype. All of the isolates in the Tn*917* group had the MLS_B phenotype. Both groups showed resistance to azithromycin but were sensitive to telithromycin.

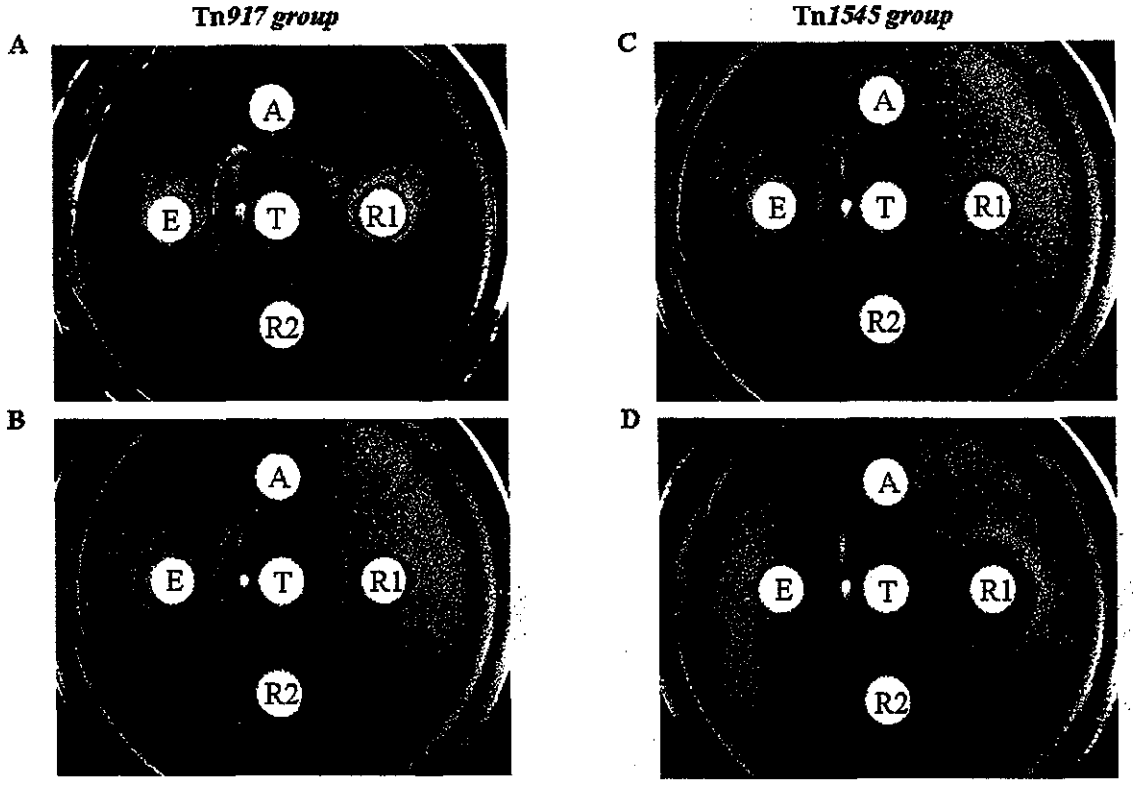

FIG. 2. Phenotype of macrolide-resistant *S. pneumoniae* strains determined by the disk diffusion method. Abbreviations: E, erythromycin (20 μg/disk); A, azithromycin (20 μg/disk), R1, rokitamycin (20 μg/disk); R2, rokitamycin (100 μg/disk); T, telithromycin (10 μg/disk). (A) MICs (in milligrams per liter) were >128 for E, A, and clindamycin; 128 for R; and 0.25 for T. (B) MICs (in milligrams per liter) were 4 for E, >128 for A and clindamycin, 8 for R, and 0.13 for T. (C) MICs (in milligrams per liter) were >128 for E, A, and clindamycin; 128 for R; and 0.25 for T. (D) MICs (in milligrams per liter) were 4 for E, >128 for A, 1 for R, 128 for clindamycin, and 0.06 for T.

TABLE 2. The five most frequent serogroups in each group of macrolide-resistant *S. pneumoniae* strains

Strains	No. (%) of isolates belonging to the following serogroup:					
	3	6	14	19	23	Others
Tn*1545* group (n = 19)	2 (10.5)	12 (63.2)	1 (5.3)	0 (0)	2 (10.5)	2 (10.5)
Tn*917* group (n = 65)	19 (29.2)	8 (12.3)	5 (7.7)	4 (6.2)	15 (23.1)	14 (21.5)

Reduction in telithromycin susceptibility. All of the strains tested showed a reduction in telithromycin susceptibility, and an inhibition zone was created by erythromycin, azithromycin, and rokitamycin. In the Tn*917* group, a square zone of inhibition was similarly formed regardless of whether erythromycin and rokitamycin MICs were high or low (Fig. 2A and B). In the Tn*1545* group, the strains with high erythromycin and rokitamycin MICs formed a square inhibition zone like that seen in the Tn*917* group, but inhibition was recognized more clearly around the rokitamycin disk (20 or 100 μg/disk), and the zone of inhibition was larger, if the erythromycin and rokitamycin MICs for the isolates were low (Fig. 2C and D).

Serogroup and genotype. Serogroup data are shown in Table 2. In the Tn*1545* group, 12 isolates (63.2%) belonged to serogroup 6. In the Tn*917* group, 19 strains (29.2%) and 15 strains (23.1%) belonged to serogroups 3 and 23, respectively, while 43 strains (47.7%) belonged to other serogroups.

PFGE results are shown in Fig. 3. In 17 strains of the Tn*1545* group, the same pattern was observed when isolates from a single geographic region were tested (Fig. 3A; Table 3). In 36 strains of the Tn*917* group, however, only a few strains showed similar patterns and most were quite different, even though the strains were isolated in the same geographical region (Fig. 3B; Table 3). These findings support the concept that Tn*1545* was spread clonally while Tn*917* was spread both clonally and horizontally.

DISCUSSION

We assessed characteristics of the macrolide resistance gene (*ermB*) in 84 clinical isolates of *S. pneumoniae* obtained from Japanese patients. The rate of macrolide resistance among *S. pneumoniae* strains isolated in Japan is 77.9%, a rate similar to that in Hong-Kong or South Korea, and 52.7% of macrolide-resistant strains possess the *ermB* gene (6). Thus, strains showing high resistance to macrolides are widespread in Japan.

In this study, the major macrolide resistance element in Japanese isolates was Tn*917* (or a Tn*917*-like element). Although it is not clear why Tn*917* is spreading among Japanese *S. pneumoniae* strains, it is possible that strains with Tn*917* are more resistant to 16-membered-ring macrolides than isolates with Tn*1545*, since macrolides with a 16-membered-ring (such as rokitamycin) are widely used in Japan.

We found the deletion of 182 bp of the Tn*917* sequence, including the −35 region of the *ermB* promoter, in all strains with Tn*917* isolated in Japan. Although the existence of a new promoter is conceivable, it could not be determined by computer simulation because we did not find a new promoter that was stronger than the putative original promoter. It is thought that these mutations have contributed to the increase in the production of the methylase, but those mechanisms have not been clarified. Although Oh et al. found a relationship between

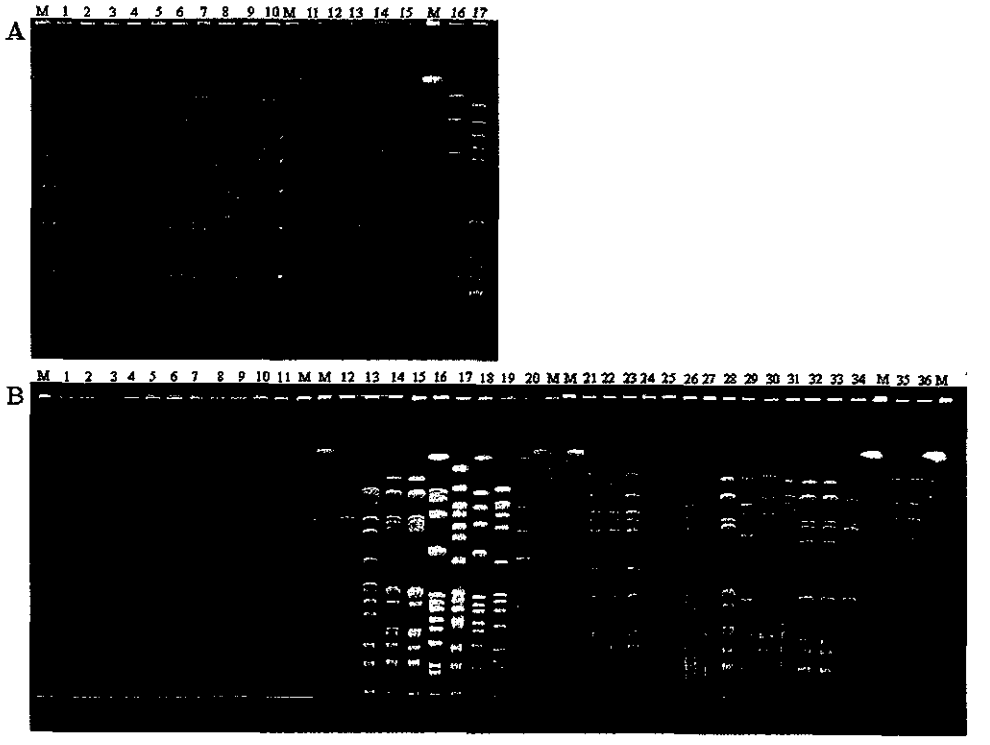

FIG. 3. PFGE of *S. pneumoniae* chromosomal DNA after digestion with the SmaI restriction enzyme. (A) Strains with Tn*1545*. (B) Strains with Tn*917*. Lanes M, lambda ladder. For details, see Table 3.

TABLE 3. PFGE results[a] for macrolide-resistant *S. pneumoniae*

Panel	Lane	Strains	Serogroup	Geographical region of isolation
A	1	KU5032	6	Kitasato
	2	KU5012	6	Kitasato
	3	KU3901	6	Kitasato
	4	KU4994	6	Kitasato
	5	KU3900	6	Kitasato
	6	KU4989	6	Kitasato
	7	KU5017	6	Kitasato
	8	KU3915	6	Kitasato
	9	KU5008	3	Kitasato
	10	KU4997	3	Kitasato
	11	B4	6	Sendai
	12	B1	6	Sendai
	13	B3	6	Sendai
	14	B5	6	Sendai
	15	A5	Other	Sendai
	16	TK9	14	Takahagi
	17	TK11	23	Takahagi
B	1	KU5197	3	Kitasato
	2	KU3784	3	Kitasato
	3	KU3781	3	Kitasato
	4	KU5019	3	Kitasato
	5	KU5003	6	Kitasato
	6	KU3800	6	Kitasato
	7	KU5213	14	Kitasato
	8	KU5020	14	Kitasato
	9	KU3791	23	Kitasato
	10	KU3785	23	Kitasato
	11	KU5203	23	Kitasato
	12	A12	6	Sendai
	13	A3	19	Sendai
	14	A13	23	Sendai
	15	A7	23	Sendai
	16	A4	Other	Sendai
	17	A2	Other	Sendai
	18	A9	Other	Sendai
	19	A8	Other	Sendai
	20	B2	Other	Sendai
	21	NU32	3	Nagasaki
	22	NU38	3	Nagasaki
	23	NU59	3	Nagasaki
	24	NU30	14	Nagasaki
	25	NU16	14	Nagasaki
	26	NU67	19	Nagasaki
	27	NU73	19	Nagasaki
	28	NU21	23	Nagasaki
	29	NU44	23	Nagasaki
	30	TK3	3	Takahagi
	31	TK1	19	Takahagi
	32	TK8	23	Takahagi
	33	TK16	23	Takahagi
	34	TK15	23	Takahagi
	35	KSM3	3	Kashima
	36	KSM4	3	Kashima

[a] Details of the experiment for which results are shown in Fig. 3, by panel and lane.

macrolide resistance and two mutations of the leader peptide in the *ermB* gene on Tn*917* from *E. faecalis* by a reporter gene assay (14), they concluded that TAAA duplication at the T591 (T421 in our data) site (which was also detected in this study) generated a translation stop codon and shortened the leader peptide by 9 amino acids so that reporter gene expression was dramatically elevated, i.e., TAAA duplication increased expression of the methylase and resulted in strong resistance to rokitamycin.

Strains that had the *ermB* gene on either transposon (or on a transposon-like sequence) showed reductions in telithromycin susceptibility in the disk diffusion test. However, for strains with Tn*1545* for which the rokitamycin MIC was lower, less telithromycin resistance was reduced by the 100-μg rokitamycin disk than for strains having Tn*917* or Tn*1545* for which rokitamycin MICs were high. In contrast, the isolates with Tn*917* showed reductions in telithromycin susceptibility induced by the 100-μg rokitamycin disk irrespective of the rokitamycin MICs. Such a result cannot be explained clearly. It has been reported that the basal level of ribosomal methylation differs from strain to strain and that the nucleotide sequence of the regulatory region shows variation in each isolate, resulting in different levels of constitutive *ermB* gene expression (24). However, we found that all strains had the same leader sequence of the *ermB* gene, even if the macrolide MICs were different. Such differences may be specific to each strain and could be based on complex mechanisms (11).

Although all strains were initially sensitive to telithromycin, the susceptibility of telithromycin was decreased by erythromycin, azithromycin, and rokitamycin (9). Because these macrolides are not used together clinically, this effect may not be a problem. In addition, there were no strains with constitutive macrolide resistance.

The PFGE patterns and serogroup distribution showed that Tn*917* spread both horizontally and clonally, while Tn*1545* spread clonally. The results of this study suggest that Tn*917* may have been transmitted from *E. faecalis* or other organisms, so that the dominant macrolide resistance gene is *ermB* on Tn*917* in Japanese pneumococci.

Recently, other mechanisms of macrolide resistance (amino acid substitutions in domain V of 23S rRNA or mutations of L4 and L22 proteins) in vitro (3, 20) and in clinical isolates (2, 15, 21) have been reported often. Kaieda et al. reported an *S. pneumoniae* strain with an *ermB* mutation that showed in vitro constitutive macrolide resistance (S. Kaieda, S., H. Yano, N. Okitsu, Y. Hosaka, R. Okamoto, H. Takahashi, and M. Inoue, Abstr. 42nd Intersci. Conf. Antimicrob. Agents Chemother., abstr. C1-1580, p. 72, 2002). It was isolated along with inducible macrolide resistance strains by culture with a disk containing 0.5 mg of telithromycin/liter, and the MIC for telithromycin was 8 mg/liter. However, the isolation rate was very low (10^{-10}), so it is thought that the appearance of mutants with constitutive resistance to macrolides, including telithromycin, is very uncommon in the clinical setting.

It is important to continue the surveillance of antimicrobial susceptibility in *S. pneumoniae* and to carefully monitor the emergence of constitutive macrolide resistance and resistance due to ribosomal mutations in *S. pneumoniae*.

ACKNOWLEDGMENTS

This work was supported in part by a grant from the COE program of the Japanese Ministry of Science, Education, and Culture and a grant from the Japanese Ministry of Health, Sports, Science, and Technology (H12-Sinko-19).

REFERENCES

1. **Appelbaum, P. C.** 1992. Antimicrobial resistance in *Streptococcus pneumoniae*: an overview. Clin. Infect. Dis. **15**:77–83.
2. **Butler, J. C., J. L. Lennox, L. K. McDougal, J. A. Sutcliffe, A. Tait-Kamradt, and F. C. Tenover.** 2003. Macrolide-resistant pneumococcal endocarditis and epidural abscess that developed during erythromycin therapy. Clin. Infect. Dis. **36**:e19–e25.

3. **Canu, A., B. Malbruny, M. Coquemont, T. Davies, P. C. Appelbaum, and R. Leclercq.** 2002. Diversity of ribosomal mutation conferring resistance to macrolides, clindamycin, streptogramin, and telithromycin in *Streptococcus pneumoniae*. Antimicrob. Agents Chemother. **46:**125–131.
4. **Courvalin, P., and C. Carlier.** 1986. Transposable multiple antibiotic resistance in *Streptococcus pneumoniae*. Mol. Gen. Genet. **205:**291–297.
5. **Doern, G. V., K. P. Heilmann, H. K. Huynh, P. R. Rhomberg, S. L. Coffman, and A. B. Brueggemann.** 2001. Antimicrobial resistance among clinical isolates of *Streptococcus pneumoniae* in the United States during 1999–2000, including a comparison of resistance rates since 1994–1995. Antimicrob. Agents Chemother. **45:**1721–1729.
6. **Farrell, D. J., I. Morrissey, S. Bakker, and D. Felmingham.** 2002. Molecular characterization of macrolide resistance mechanisms among *Streptococcus pneumoniae* and *Streptococcus pyogenes* isolated from the PROTEKT 1999–2000 study. J. Antimicrob. Chemother. **50**(Suppl. S1):39–47.
7. **Gay, K., W. Baughman, Y. Miller, D. Jackson, C. G. Whitney, A. Schuchat, M. M. Farley, F. Tenover, and D. S. Stephens.** 2000. The emergence of *Streptococcus pneumoniae* resistant to macrolide antimicrobial agents: a 6-year population-based assessment. J. Infect. Dis. **182:**1417–1424.
8. **Gillespie, S. H., C. Ullman, M. D. Smith, and V. Emery.** 1994. Detection of *Streptococcus pneumoniae* in sputum samples by PCR. J. Clin. Microbiol. **32:** 1308–1311.
9. **Kaieda, S., N. Okitsu, H. Yano, Y. Hosaka, R. Nakano, R. Okamoto, H. Takahashi, and M. Inoue.** 2003. Induction of telithromycin resistance in *Streptococcus pneumoniae*. J. Antimicrob. Chemother. **52:**736–737.
10. **Leclercq, R., and P. Courvalin.** 1991. Bacterial resistance to macrolide, lincosamide, and streptogramin antibiotics by target modification. Antimicrob. Agents Chemother. **35:**1267–1272.
11. **Leclercq, R., and P. Courvalin.** 2002. Resistance to macrolides and related antibiotics in *Streptococcus pneumoniae*. Antimicrob. Agents Chemother. **46:** 2727–2734.
12. **Martin, P., P. Trieu-Cuot, and P. Courvalin.** 1986. Nucleotide sequence of the *tetM* tetracycline resistance determinant of the streptococcal conjugative shuttle transposon Tn*1545*. Nucleic Acids Res. **14:**7047–7058.
13. **National Committee for Clinical Laboratory Standards.** 1999. Performance for antimicrobial susceptibility testing; ninth informational supplement, M100-S9, vol. 19. National Committee for Clinical Laboratory Standards, Wayne, Pa.
14. **Oh, T.-G., A. R. Kwon, and E.-C. Choi.** 1998. Induction of *ermAMR* from a clinical strain of *Enterococcus faecalis* by 16-membered-ring macrolide antibiotics. J. Bacteriol. **180:**5788–5791.
15. **Pihlajamaki, M., J. Ktaja, H. Seppala, J. Elliot, M. Leinonen, P. Huovinen, and J. Jalava.** 2002. Ribosomal mutation in *Streptococcus pneumoniae* clinical isolates. Antimicrob. Agents Chemother. **46:**654–658.
16. **Ruoff, K. L., R. A. Whiley, and D. Beighton.** 1999. *Streptococcus*, p. 283–296. *In* P. R. Murray, E. J. Baron, M. A. Pfaller, F. C. Tenover, and R. H. Yolken (ed.), Manual of clinical microbiology, 7th ed. ASM Press, Washington, D.C.
17. **Shaw, J. H., and D. B. Clewell.** 1985. Complete nucleotide sequence of macrolide-lincosamide-streptogramin B resistance transposon Tn*917* in *Streptococcus faecalis*. J. Bacteriol. **164:**782–796.
18. **Sutcliffe, J., T. Grebe, A. Tait-Kamradt, and L. Wondrack.** 1996. Detection of erythromycin-resistant determinants by PCR. Antimicrob. Agents Chemother. **40:**2562–2566.
19. **Tait-Kamradt, A., J. Clancy, M. Cronan, F. Dib-Hajj, L. Wondrack, W. Yuan, and J. Sutcliffe.** 1997. *mefE* is necessary for the erythromycin-resistant M phenotype in *Streptococcus pneumoniae*. Antimicrob. Agents Chemother. **41:**2251–2255.
20. **Tait-Kamradt, A., T. Davies, M. Cronan, M. R. Jacobs, P. C. Appelbaum, and J. Sutcliffe.** 2000. Mutations in 23S rRNA and ribosomal protein L4 account for resistance in pneumococcal strains selected in vitro by macrolide passage. Antimicrob. Agents Chemother. **44:**2118–2125.
21. **Tait-Kamradt, A., T. Davis, P. C. Appelbaum, F. Depardieu, P. Courvalin, J. Petitpas, L. Wondrack, A. Walker, M. R. Jacobs, and J. Sutcliffe.** 2000. Two new mechanisms of macrolide resistance in clinical strains of *Streptococcus pneumoniae* from Eastern Europe and North America. Antimicrob. Agents Chemother. **44:**3395–3401.
22. **Trieu-Cuot, P., C. Poyart-Salmeron, C. Carlier, and P. Courvalin.** 1990. Nucleotide sequence of the erythromycin resistance gene of the conjugative transposon Tn*1545*. Nucleic Acids Res. **18:**3660.
23. **Yano, H., M. Suetake, A. Kuga, K. Irinoda, R. Okamoto, T. Kobayashi, and M. Inoue.** 2000. Pulsed-field gel electrophoresis analysis of nasopharyngeal flora in children attending a day care center. J. Clin. Microbiol. **38:**625–629.
24. **Zhong, P., Z. Cao, R. Hammond, Y. Chen, J. Beyer, V. D. Shortridge, L. Y. Phan, S. Pratt, J. Capobianco, K. A. Reich, R. K. Flamm, Y. S. Or, and L. Katz.** 1999. Induction of ribosome methylation in MLS-resistant *Streptococcus pneumoniae* by macrolides and ketolides. Microb. Drug Resist. **5:**183–188.

Comparative Study of the Inhibition of Metallo-β-Lactamases (IMP-1 and VIM-2) by Thiol Compounds That Contain a Hydrophobic Group

Wanchun JIN,[a] Yoshichika ARAKAWA,[b] Hisami YASUZAWA,[a] Tomoko TAKI,[a] Ryo HASHIGUCHI,[a] Kana MITSUTANI,[a] Asumi SHOGA,[a] Yoshihiro YAMAGUCHI,[a] Hiromasa KUROSAKI,[a] Naohiro SHIBATA,[b] Michio OHTA,[c] and Masafumi GOTO*,[a]

[a] *Graduate School of Pharmaceutical Sciences, Kumamoto University; 5–1 Oe Honmachi, Kumamoto 862–0973, Japan:* [b] *Department of Bacterial Pathogenesis and Infection Control, National Institute of Infectious Diseases; 4–7–1 Gakuen, Musashi-Murayama, Tokyo 208–0011, Japan: and* [c] *Department of Bacteriology, Nagoya University School of Medicine; 65 Tsurumai-cho, Showa-ku, Nagoya 466–8550, Japan.* Received January 14, 2004; accepted March 9, 2004

For the purpose of screening of inhibitors that are effective for wide range of metallo-β-lactamases, the inhibitory effect of two series of compounds, 2-ω-phenylalkyl-3-mercaptopropionic acid (PhenylC*n*SH (*n*=1—4)) and *N*-[(7-chloro-quinolin-4-ylamino)-alkyl]-3-mercapto-propionamide (QuinolineC*n*SH (*n*=2—6)), where *n* denotes the alkyl chain length, on metallo-β-lactamases IMP-1 and VIM-2 was examined. These inhibitors contain a thiol group and a hydrophobic group linked by variable-length methylene chain. PhenylC*n*SH (*n*=1—4) was found to be a potent inhibitor of both IMP-1 and VIM-2. PhenylC4SH was the potent inhibitor of both IMP-1 (IC_{50}=1.2 μM) and VIM-2 (IC_{50}=1.1 μM) among this study. When the number of methylene units was varied, QuinolineC4SH showed the maximum inhibitory activity against IMP-1 and VIM-2 (IC_{50}=2.5 μM and IC_{50}=2.4 μM). The relationship between the inhibitory effect of the alkyl chain length was different for both series of inhibitors, suggesting that IMP-1 has a tighter binding site than VIM-2. QuinolineCnSH did not serve as a fluorescence reagent for metallo-β-lactamases.

Key words metallo-β-lactamase; inhibitor; thiol; zinc; 3-mercaptopropionic acid

A wide variety of β-lactam antibiotics are used in the treatment of infectious diseases. These antibiotics block the cell wall biosynthesis of bacteria by inhibiting a transpeptidase. However, bacteria have developed several strategies for resisting β-lactam antibiotics, including the production of a family of enzymes, β-lactamases. The β-lactamases catalyze the hydrolysis of β-lactam antibiotics, opening the β-lactam ring and rendering the antibiotics inactive.[1—3]

β-Lactamases have been grouped into four molecular classes, A, B, C and D, based on their amino-acid sequence homologies by Ambler *et al.*[4] Those that belong to classes A, C and D are serine-β-lactamases which use serine as the active site to facilitate catalysis, and those that belong to class B are metallo-β-lactamases (MBLs) that contain one or two zinc ions at the active site to facilitate β-lactam cleavage. Based on the difference in their primary structures, MBLs have been classified into three subfamilies,[5] B1 (BcII from *Bacillus cereus*,[6] CcrA from *Bacteroides fragilis*,[7] IMP-1 from *Serratia marcescens*,[8] VIM-2 from *Pseudomonas aeruginosa*[9]), B2 (CphA from *Aeromonas hydrophila* AE036[10]), and B3 (L1 from *Stenotrophomonas maltophilia*[11]). MBLs are able to hydrolyze most of the β-lactam antibiotics[6—11] and pose a serious clinical threat because of their ability to degrade carbapenems including imipenem and meropenem, which are not degraded by most serine-β-lactamases.[1—3]

The genes that encode IMP-1 and VIM-2 have been found to be located in plasmids that are horizontally transferable to other bacteria[8] and no clinically available inhibitors for them exist at present.

IMP-1 consists of an αβ/βα motif, and two Zn(II) ions are located at the bottom of a wide shallow groove between the β-sheets.[12] One of the Zn(II) ions is coordinated by three histidine residues (3H site), and the other is coordinated by His, Asp, Cys residues and water-2 molecule (DCH site). In addition, the water-1 molecule would be expected to bridge the two Zn(II) ions presumably in the form of a hydroxide ion, although this is not confirmed in the three-dimensional structure of IMP-1 but is based on the three-dimensional structure of CcrA (PDB 1ZNB).[13]

VIM-2 was isolated from *Pseudomonas aeruginosa* in 1996 in France,[9] and has also been identified recently in Japan.[14] On the basis of amino acid sequences, 31% of the residues are identical in these enzymes, indicating that VIM-2[9] and IMP-1[8] retain the binuclear metal binding motif where Zn(II) ions are coordinated by the side chains of conserved amino acids. The amino acid sequences of a flexible loop, a β-sheet flap, which is thought to be important in the binding of particular inhibitors and substrates, are different between IMP-1 and VIM-2 especially in the nature and position of the hydrophobic amino acid: Trp28 which is located in the edge of the flap in the case of IMP-1 but is replaced with Ala in VIM-2.

A number of compounds have been examined as inhibitors of MBLs since 1996, including trifluoromethyl alcohols and ketones,[15] hydroxamates,[16] thiols,[17—25] thioester derivatives,[19,26—29] cysteinyl peptides,[30] biphenyl tetrazoles,[31,32] mercaptocarboxylates,[12,21,29] 1β-methylcarbapenem derivatives,[33,34] 2,3-disubstituted succinic acid derivatives,[35] tricyclic natural products,[36] sulfonyl hydrazones,[37] and a synthetic cephamycin.[38] Most of these compounds, however, have been shown to exert their adverse effects only on a limited number of MBLs.

The X-ray crystal structures of MBLs complexed with inhibitors have been reported, including CcrA-4-morpholineethanesulfonic acid,[39] CfiA-tricyclic natural products,[36] IMP-1-mercaptocarboxylate,[12] 2,3-disubstituted succinic acid derivatives,[35] BlaB-D-captopril,[40] and FEZ-D-captopril.[41] From these reports, these enzymes have conserved the amino acid residues and the binuclear metal center at the ac-

* To whom correspondence should be addressed. e-mail: gmphiwin@gpo.kumamoto-u.ac.jp

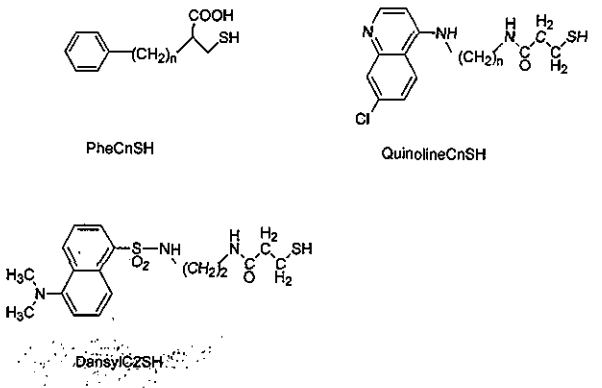

Fig. 1. Chemical Structures of Inhibitors Used in This Study

tive site. There are various combinations with respect to the enzyme-inhibitor binding. MBLs offer an opportunity for the structure-aided design of inhibitors as well as a better understanding of structure–activity relationships.

In 1997, we reported that mercaptocarboxylic acids are potent inhibitors of IMP-1.[17] The thiol group of inhibitors was assumed to coordinate with the metal ions in the active site, and this was supported by an X-ray crystallographic analysis of 2-[5-(1-tetrazolyl-methyl)thien-3-yl]-*N*-[2-(mercaptomethyl)-4-(phenylbutyrylglycine)] and the IMP-1 complex.[12]

A fluorescent probe of IMP-1 having a dansyl and a thiol group, DansylC2SH, has recently been reported by our group.[25] The fluorescent probe also functions as a potent inhibitor of IMP-1. The dansyl group appears to interact with hydrophobic groups near the active site of IMP-1.

In this study, we used three functional groups to strengthen the interactions with MBLs: a thiol group, presumed to bind with Zn(II) ions, an aromatic ring to bind with the hydrophobic pocket, and a carboxyl group to interact *via* hydrogen bonding or electrostatic interactions with conserved residues, such as Lys. Three types of compounds that contain the three functional groups above, PhenylCnSH, QuinolineCnSH, and DansylC2SH shown in Fig. 1 were examined as inhibitors of IMP-1 and VIM-2.

MATERIALS AND METHODS

Materials The bla_{IMP} gene is derived from *S. marcescens* TN9160[42] and was cloned into pKF19k (denoted as pKF19k/IMP). The construction of pKF19k/IMP will be reported elsewhere.[43] The *P. aeruginosa* strain NCB326 was isolated from the drainage fluid of a liver abscess patient in 1999 in Nara, Japan. *Bam*HI digested fragments of whole-cell DNA from *P. aeruginosa* NCB326 were ligated into the *Bam*HI-restricted plasmid pBCSK(+) (Stratagene, La Jolla, Calif., U.S.A.). Recombinant plasmids were introduced by electroporation into *E. coli* HB101 competent cells. *E. coli* NCB326-1B2 carried a recombinant plasmid pVM4k (named pVM4k/VIM-2) and this transformant successfully produced a VIM-2 metallo-β-lactamase.

Construction of Expression Vectors, pET9a/IMP The over-expression of IMP-1 metallo-β-lactamase in *E. coli* was achieved as follows: the bla_{IMP} gene without the nucleotide coding the signal peptide was amplified using two primers IMP-NdeI (5′-TTCCTTTCATATggCAgAgTCTTTgCCAgATTT-3′), which was designed to add *Nde*I linker (underlined), and IMP-BamHI (5′-gTTggATCCTAgAAATTTAgTTgCTTggTTTTgATggT-3′), designed to add the *Bam*HI linker (underlined). PCR was performed with 350 ng of template DNA (plasmid pKF19k/IMP), 50 pmol of each primer, 2.5 U of *taq* DNA polymerase (TaKaRa Bio INC., Shiga, Japan) in a final volume 100 μl in the buffer system provided by the manufacturer. The resulting PCR product was digested with *Nde*I and *Bam*HI and cloned in pET9a (Novagen, Madison, Wis.), digested with the same enzymes, to give the recombinant plasmid. The constructed expression vectors, denoted as pET9a/IMP, were introduced into *E. coli* BL21 (DE3) (Novagen).

Expression and Purification of the IMP-1 Enzymes *E. coli* BL21 (DE3), carrying plasmids pET9a/IMP, was cultured in 10 l of LB broth supplemented with kanamycin (50 μg/ml). At an Abs_{600} of 3, isopropyl-β-D-thiogalactopyranoside (IPTG) was added, at final concentration of 1 mM, and the culture was further incubated for 8 h. Cells were harvested by centrifugation and suspended in 30 ml of 50 mM phosphate buffer (pH 7.0, containing 100 μM $Zn(NO_3)_2$) and disrupted by sonication (60 cycles, each cycle for 5 s at 1 min intervals), then centrifuged at 150000×***g*** for 60 min at 4 °C. The cleared supernatant was used in the subsequent chromatographic purification, as described previously.[44] The purity of the enzyme was verified by sodium dodecyl sulfate polyacrylamide gel electrophoresis (SDS-PAGE) and Coomassie blue staining. Final preparation showed a single band with more than 95% purity.

Production and Purification of VIM-2 VIM-2 was expressed by *E. coli* NCB326-1B2 harboring pVM4k/VIM-2 and purified using methods described by Poirel *et al.* in 2000.[9]

E. coli NCB326-1B2 carrying plasmids pVM4k/VIM-2 was cultured in 10 l of LB broth supplemented with ABPC (50 μg/ml). The culture was incubated for 12 h at 37 °C (Abs_{600} was 1.0). Cells were harvested by centrifugation and suspended in 30 ml of 50 mM Bis-Tris buffer (pH 6.5, containing 10 μM $Zn(NO_3)_2$) and disrupted by sonication (60 cycles, each cycle for 5 s in a minite), then centrifuged at 150000×***g*** for 60 min at 4 °C. The cleared supernatant was used in the subsequent chromatographic purification. Anion-exchange chromatography was performed on a Q-Sepharose Fast Flow (Pharmacia Biotech, Uppsala, Sweden, ϕ26 mm×100 mm) preequilibrated with 50 mM Bis-Tris buffer (pH 6.5, containing 10 μM $Zn(NO_3)_2$) and was eluted with a linear gradient of 0 to 0.3 M NaCl in 50 mM Bis-Tris buffer (pH 6.5, containing 10 μM $Zn(NO_3)_2$). Fractions containing β-lactamase activity were collected, concentrated and the buffer changed to 50 mM phosphate buffer (pH 7.0, containing 2 μM $Zn(NO_3)_2$) containing 0.3 M NaCl, were applied to a gel-filtlation column, Sephadex G-75 (Pharmacia Biotech, Uppsala, Sweden, ϕ50 mm×800 mm), preequilibrated with 50 mM phosphate buffer (pH 7.0, containing 2 μM $Zn(NO_3)_2$) containing 0.3 M NaCl. The purified enzyme was used in subsequent β-lactamase assays. The purity of the preparation was checked by SDS-PAGE, and final preparation showed a single band with more than 95% purity. The molecular weight of purified VIM-2, M_r=29.7 kDa as SDS-PAGE, was in agreement with the reported value.[9]

Assays of Substrate Hydrolysis of IMP-1 and VIM-2 A spectrophotometric method was used to measure the initial

rate of consumption of a chromophoric substrate, nitrocefin, by IMP-1 (VIM-2). A solution (3.1 ml) of nitrocefin (100 μM) in 50 mM Tris–HCl buffer (pH 7.4, 0.5 M NaCl) was incubated at 30 °C for 5 min. The enzyme solution of 0.4 μM IMP-1 (VIM-2) (10 μl) was added to the substrate solution and the increase in absorbance at 491 nm ($\Delta\varepsilon$=20000) was recorded. Enzymic rate parameters, K_m and k_{cat}, were determined by a nonlinear least-squares method (Kaleida graph) to fit the Michaelis–Menten equation.

Determination of IMP-1 and VIM-2 The concentrations of IMP-1 and VIM-2 were determined from the absorbance at 280 nm: ε_{280}=49000 $M^{-1}cm^{-1}$ for IMP-1 and ε_{280}=32000 $M^{-1}cm^{-1}$ for VIM-2.

PhenylC*n*SH (*n*=1—4) PhenylC*n*SH (*n*=1—4) were prepared using a method described by Park J. D. *et al.*[45]

QuinolineC3SH, *N*-[3-(7-Chloro-quinolin-4-ylamino)-propyl]-3-mercapto-propionamide 4,7-Dichloroquinoline (1.64 g, 0.0083 mol) was added to 1,3-diaminopropane (6.15 g, 0.083 mol). After refluxing at 100 °C for 4 h, the mixture was concentrated to give the crude product, which was chromatographed with a Wakogel C-300 (Silica Gel) column by elution with methanol : chloroform : 28% aqueous ammonia=40 : 360 : 1 to give a yellow solid (1.65 g, 84.5%).

To the yellow solid (1.54 g, 0.0065 mol) and BPO reagent (benzotriazol-1-yloxytris-(dimethylamino) phosphonium hexafluorophosphate) (2.88 g, 0.0065 mol) dissolved in 150 ml of chloroform, 3-mercaptopropionic acid (0.69 g, 0.0065 mol) and triethylamine (1.76 g, 0.017 mol) were added. The mixture was stirred under argon at room temperature overnight and concentrated under reduced pressure to give a pale yellow solid. This was purified by Wakogel C-300 (Silica Gel) column chromatography eluted with the solution containing methanol, chloroform, and 28% aqueous ammonia (40 : 360 : 1) to give a white solid. (0.71 g, 33.9%). ^{1}H-NMR ($CDCl_3$): δ 1.26 (t, 1H), 1.92 (q, 2H), 2.18 (s, 1H), 2.57 (t, 2H), 2.82 (t, 2H), 3.38 (t, 2H), 3.51 (t, 2H), 6.57 (d, 1H, J=6.71 Hz), 7.47 (d, 1H, J=1.83 Hz), 7.74 (s, 1H), 8.13 (d, 1H, J=9.15 Hz), 8.23 (d, 1H, J=6.71 Hz). ^{13}C-NMR ($CDCl_3$): δ 20.48, 27.97, 36.55, 40.08, 40.39, 98.55, 116.37, 122.35, 123.68, 127.10, 138.41, 142.37, 145.79, 154.04, 173.15. HR-FAB-MS: *m/z* 323.0847 [Calcd for $C_{15}H_{18}N_3OSCl$ (M^+) 323.0859].

QuinolineC*n*SH (*n*=2, 4—6) These compounds were synthesized, as described for the synthesis of QuinolineC3SH, as described above. A flow chart of the synthesis is shown in Chart 1.

QuinolineC2SH, *N*-[2-(7-Chloro-quinolin-4-ylamino)-ethyl]-3-mercapto-propionamide Yield, 13.8%. ^{1}H-NMR ($CDCl_3$): δ 1.24 (t, 1H), 2.59 (t, 2H), 2.78 (t, 2H), 3.64 (t, 2H), 3.7 (q, 2H), 6.7 (d, 1H), 7.58 (d, 1H), 7.73 (s, 1H), 8.12 (d, 1H), 8.19 (d, 1H). ^{13}C-NMR ($CDCl_3$): δ 38.04, 39.52, 45.62, 47.29, 98.46, 115.33, 119.58, 124.12, 127.98, 138.63, 140.00, 142.76, 155.78, 174. HR-FAB-MS: *m/z* 309.0684 [Calcd for $C_{14}H_{16}N_3OSCl$ (M^+) 309.0703].

QuinolineC4SH, *N*-[4-(7-Chloro-quinolin-4-ylamino)-butyl]-3-mercapto-propionamide Yield, 27.1%. ^{1}H-NMR ($CDCl_3$): δ 1.22 (t, 1H), 1.54 (q, 2H), 1.74 (q, 2H), 2.48 (t, 2H), 2.78 (t, 2H), 3.24 (t, 2H), 3.30 (t, 2H), 6.38 (d, 1H, J=5.49 Hz), 7.34 (d, 1H, J=7.33 Hz), 7.86 (s, 1H), 7.87 (d, 1H, J=4.88 Hz), 8.39 (d, 1H, J=5.5 Hz). ^{13}C-NMR ($CDCl_3$): δ 20.51, 26.61, 29.48, 39.27, 40.31, 43.01, 98.85, 117.45, 122.09, 125.37, 127.59, 135.36, 148.65, 150.85, 151.45, 171.72.

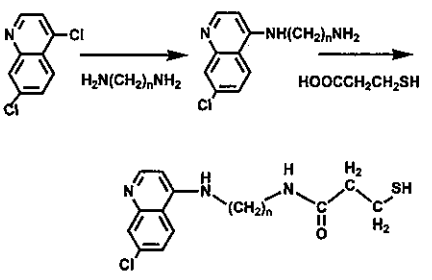

Chart 1. Synthetic Route of QunolineC*n*SH (*n*=2—6)

QuinolineC5SH, *N*-[5-(7-Chloro-quinolin-4-ylamino)-pentyl]-3-mercapto-propionamide Yield, 57.3%. ^{1}H-NMR ($CDCl_3$): δ 1.20 (t, 1H) 1.51 (q, 2H), 1.61 (q, 2H), 1.80 (q, 2H), 2.48 (t, 1H), 2.76 (t, 2H), 3.24 (t, 2H), 3.37 (t, 1H), 3.38 (t, 2H), 6.49 (d, 1H, J=5.49 Hz), 7.40 (d, 1H, J=9.16 Hz), 7.80 (s, 1H), 8.09 (d, 1H, J=9.15 Hz), 8.33 (d, 1H, J=5.49 Hz). ^{13}C-NMR ($CDCl_3$): δ 20.84, 24.95, 28.50, 29.75, 39.74, 40.64, 43.68, 99.19, 117.99, 123.73, 126.01, 136.55, 147.89, 150.63, 152.73, 173.13. HR-FAB MS: *m/z* 351.1139 [Calcd for $C_{17}H_{22}N_3OSCl$ (M^+) 351.1172].

QuinolineC6SH, *N*-[6-(7-Chloro-quinolin-4-ylamino)-hexyl]-3-mercapto-propionamide Yield, 50.4%. ^{1}H-NMR ($CDCl_3$): δ 1.24 (t, 1H), 1.48 (q, 2H), 1.52 (q, 2H), 1.66 (q, 2H), 1.78 (q, 2H), 2.50 (t, 2H), 2.79 (t, 2H), 3.29 (t, 2H), 3.35 (t, 2H), 6.39 (d, 1H, J=6.10 Hz), 7.35 (d, 1H, J=6.71 Hz), 7.83 (s, 1H), 7.97 (d, 1H, J=8.55 Hz), 8.34 (d, 1H, J=5.5 Hz). ^{13}C-NMR ($CDCl_3$): δ 19.44, 25.38, 25.54, 27.41, 28.41, 35.71, 38.20, 39.24, 41.94, 97.78, 116.38, 121.02, 124.30, 126.52, 134.29, 147.58, 149.78, 150.38, 170.65. HR-FAB-MS: *m/z* 365.1274 [Calcd for $C_{18}H_{24}N_3OSCl$ (M^+) 365.1329].

Inhibition of IMP-1 and VIM-2 A portion of 0.1 ml of an inhibitor [PhenylC*n*SH (*n*=1—4), DansylC*n*SH (*n*=2), QuinolineC*n*SH (*n*=2—6)] at various concentrations in methanol and 0.01 ml of 310 nM enzyme (IMP-1 and VIM-2) in 50 mM Tris–HCl (pH 7.4, 0.5 M NaCl) was added to 2.9 ml of 50 mM Tris–HCl buffer (pH 7.4, 0.5 M NaCl). The enzyme–inhibitor mixture was incubated for 10 min at 30 °C, and a 0.1 ml DMSO solution of 3.1 mM nitrocefin was then added and the absorbance change at 491 nm monitored for 3 min. Methanol was used instead of an inhibitor as a control.

The molar activity, k_2/min^{-1}, was determined from the initial velocity, v, by v/[E], and plotted against the concentration of the inhibitors. IC_{50} values were determined from this and K_i values were determined by fitting k_2 to a competitive inhibition of Eq. 1 using K_m values of 20 μM and 22.5 μM for IMP-1 and VIM-2 respectively,

$$k_2 = \frac{V_{max}[S]}{K_m\left(1+\frac{[I]}{K_i}\right)+[S]} \quad (1)$$

where, k_2: molar activity, $k_{2max}=V_{max}/[E]$, V_{max}=the maximum velocity.

Fluorescence Titration of IMP-1 with QuinolineC*n*SH (*n*=2—6) The method used to examine fluorescence reported by Kurosaki *et al.*[25] was used in this experiment. Flu-

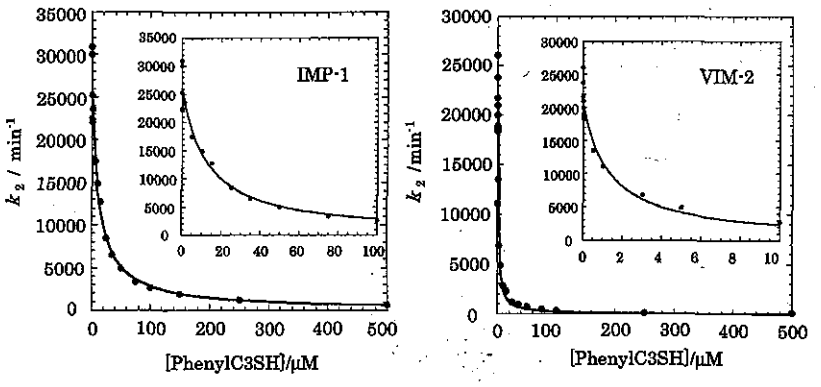

Fig. 2. Typical Plots of Molar Activity of IMP-1 (Left) and VIM-2 (Right) against the Concentration of PhenylC3SH

orescence spectra were measured at 25 °C, with a 5.0 nm of slit width, using 1 μM of QuinolineC*n*SH (n=2—6) as a fluorescence agent with an excitation of 340 nm and 280 nm using 50 mM Tris–HCl buffer (pH 7.4, 0.5 M NaCl) containing 10% of methanol.

RESULTS

K_i (Inhibition Constant) and IC_{50} (50% Inhibitory Concentration) of Inhibitors agaist IMP-1 and VIM-2 Using nitrocefin as a substrate, the molar activity k_2/min^{-1} in the presence of each inhibitor was obtained from the initial rate measurement and was plotted against the concentration of each inhibitor, (PhenylC*n*SH (n=1—4), DansylC*n*SH (n=2), and QuinolineC*n*SH (n=2—6)). Typical plots are shown in Fig. 2 (IMP-1 and VIM-2). Values for the IC_{50} of IMP-1 and VIM-2 were calculated from these concentration response curves. Inhibition constants, K_i, were determined by fitting the kinetic data to that for the competitive inhibition using Eq. 1.

Inhibition by PhenylC*n*SH (n=1—4) PhenylC*n*SH (n=1—4) were synthesized and tested as inhibitors of carboxypeptidase A (CPA), a Zn(II) enzyme, by Park *et al.*[45] The IC_{50} and K_i values for IMP-1 and VIM-2 are listed in Table 1.

The IC_{50}s for IMP-1 were found to be in a range between 1.2 μM (PhenylC4SH) and 16.4 μM (PhenylC1SH), and the inhibition constants, K_i, had values between 0.21 μM (PhenylC4SH) and 2.78 μM (PhenylC1SH). When the number of methylene units in the linker was varied, PhenylC4SH was found to inhibit IMP-1 more strongly among PhenylC*n*SH (n=1—4). 3-Mercaptopropionic acid has been reported to have a K_i value of 1.2 μM to IMP-1.[17] In comparison, PhenylC4SH was found to be a more potent inhibitor.

IC_{50} values for VIM-2 were found to be in a range between 1.1 μM (PhenylC4SH) and 14.3 μM (PhenylC1SH). The inhibition constants, K_i, have values between 0.19 μM (PhenylC4SH) and 2.36 μM (PhenylC1SH). PhenylC*n*SH (n=1—4) were found to be potent inhibitors of VIM-2 as well as of IMP-1. When the number of methylene units of the linker was varied, PhenylC3SH and PhenylC4SH was also the potent inhibitor of VIM-2.

PhenylC*n*SH (n=1—4) were found to be potent inhibitor for both IMP-1 and VIM-2, and a comparison of the inhibition constant K_i for PhenylC*n*SH (n=1—4) for IMP-1 and VIM-2 is shown in Fig. 3. The dependency of the inhibitory effect on the number of methylene units of the linker, n, is different for IMP-1, compared to VIM-2. PhenylC4SH inhibits both IMP-1 and VIM-2 more strongly and PhenylC1SH the most weakly. VIM-2 is as susceptible when n=2 and n=3 as n=4 but the susceptibility of IMP-1 is significant only for n=4.

Table 1. IC_{50} and K_i Values for PhenylC*n*SH (n=1—4) and Quinoline C*n*SH (n=2—6) to IMP-1 and VIM-2

Inhibitors	IC_{50}/μM	
	IMP-1	VIM-2
PhenylC1SH	16.4	14.3
PhenylC2SH	7.4	2.6
PhenylC3SH	9.7	1.3
PhenylC4SH	1.2	1.1
QuinolineC2SH	14.2	6.3
QuinolineC3SH	6.6	6.5
QuinolineC4SH	2.5	2.4
QuinolineC5SH	6.7	7.6
QuinolineC6SH	3.4	4.9

Inhibition by a Fluorescent Probe, DansylC*n*SH (n=2) A fluorescent probe, DansylC2SH for IMP-1, containing a thiol group and a dansyl group was synthesized, and reported as potent inhibitor for IMP-1.[25] DansylC2SH (n=2) inhibited IMP-1 and VIM-2: the IC_{50} values were 2.3 μM and 5.2 μM, the inhibition constant K_i was 0.42 μM and 1.1 μM for VIM-2 and IMP-1.[25]

QuinolineC*n*SH (n=2—6) An increase in fluorescence intensity was found on the addition of IMP-1 to DansylC2SH, but the addition of IMP-1 to QuinolineC*n*SH led to a decrease in fluorescence intensity. A comparison of structures of QuinolineC*n*SH and with that of DansylC2SH shows that the sulfonyl group between the quinoline group, a fluorescence group, and the HN group is missing in Quinoline*C*n*SH*.

The IC_{50} and K_i values for IMP-1 and VIM-2 are listed in Table 1.

QuinolineC*n*SH (n=2—6) act as effective inhibitors against IMP-1 and VIM-2. The IC_{50} for IMP-1 was found to be in a range between 2.5 μM (QuinolineC4SH) and 14.2 μM (QuinolineC2SH). The inhibition constants, K_i, have values between 0.44 μM (QuinolineC4SH) and 2.97 μM (QuinolineC2SH). The IC_{50} for VIM-2 was found to be in a range between 2.4 μM (QuinolineC4SH) and 7.6 μM (QuinolineC5SH). The inhibition constants, K_i, have values between

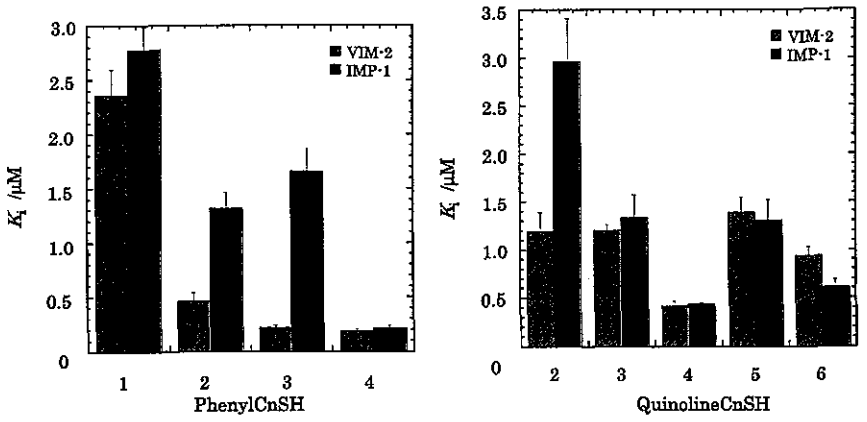

Fig. 3. Variation of Inhibition Constants of IMP-1 and VIM-2 with n, for PhenylCnSH (Left) and QuinolineCnSH (Right)

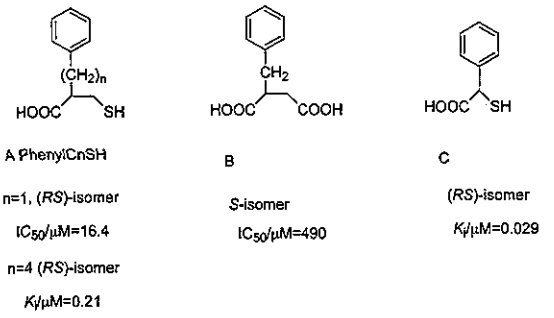

Fig. 4. Relation of Inhibitory Effect *versus* Structures, for Several Inhibitors of IMP-1

0.42 μM (QuinolineC4SH) and 1.39 μM (QuinolineC5SH). When the number of methylene units was varied, QuinolineC4SH showed the maximum inhibitory activity against both IMP-1 and VIM-2, as shown in Fig. 3. The magnitude of K_i decreased with the number of methylene units from 2 to 4 for IMP-1, but remained unchanged for VIM-2.

DISCUSSION

PhenylCnSH (n=1—4) and QuinolineCnSH (n=2—6) are found to be potent inhibitors for MBLs in this study.

The following interactions of PhenylCnSH (n=1—4) with IMP-1 and VIM-2 would be predicted: 1) replacement of the water-1 between the two Zn(II) ions with the thiol group in the active site, 2) hydrogen bonding of the oxygen of the carboxyl group with amino acids of the enzyme or replacement of water-2 coordinated to the Zn(II) ion in the DCH site, 3) hydrophobic interactions between the phenyl group and the hydrophobic pockets of MBLs.

1) The thiol group of PhenylCnSH (n=1—4) inhibitors appears to bind with Zn(II) ions of the active site of MBLs. This was supported by the X-ray crystallographic analysis of a complex of IMP-1 with a thiol compound.[12]

2) The phenyl group of PhenylCnSH (n=1—4) may interact with hydrophobic amino acid(s) near the active site. The phenyl ring of PhenylC4SH is located at a sufficient distance to effect hydrophobic interactions with a hydrophobic pocket near the active site of IMP-1. PhenylC3SH and PhenylC4SH inhibit both IMP-1 and VIM-2 more strongly, and PhenylC2SH was found to strongly inhibit VIM-2 to a greater extent than IMP-1. These results suggest that the hydrophobic pocket of VIM-2 is larger than IMP-1, and is located near the Zn(II) site. PhenylC1SH showed only a weak inhibition for VIM-2. When the number of methylene units is 3 and 4, it can be considered to be a suitable distance for interacting with the hydrophobic pocket of VIM-2 (Fig. 3).

For the case of the inhibition of CPA by PhenylCnSH (n=1—4), the K_i of PhenylCnSH (n=1—4) was determined to be 0.010, 2.1, 1.35, and 1.3 μM respectively.[45] PhenylC1SH inhibits CPA most strongly by electrostatic interactions between the oxygen of the carboxyl group and the ionic side chain of CPA as well as binding of the thiol with Zn(II) and hydrophobic interactions. Although PhenylC4SH inhibited most strongly, the K_i values for IMP-1 and VIM-2 are not greatly different from the others with respect to CPA. The observation that PhenylCnSH (n=1—4) inhibited both of IMP-1 and VIM-2 indicates that these compounds are inhibitors of other MBLs.

A comparison of the inhibition constants and structures of other inhibitors are shown in Fig. 4.

Although only the thiol group of PhenylC1SH is replaced with a carboxyl group for inhibitor B, a 2,3-disubstituted succinic acid, reported by Toney[35] a large difference in the IC_{50}: 16.4 μM was found for PhenylC1SH and 490 μM by B for IMP-1 when the substrate was nitorocefin. This suggests that a thiol group is a very important group in terms of inhibiting MBLs. PhenylC4SH was the potent inhibitor of IMP-1 among the PhenylCnSH series. However, Mollard reported that inhibitor C has a K_i value of 29 nM[23] lower by 10 fold than PhenylC4SH. We have reported that mercaptoacetic acid is a reversible inhibitor with a K_i of 0.23 μM.[17] Inhibitor C having the phenyl group on C2 position of mercaptoacetic acid led to approximately 10 fold high activity compared to mercaptoacetic acid. This higher K_i may reflect much higher hydrophobic Toney *et al.* have reported that the addition of the benzyl group at C3 position of inhibitor B increases K_i by 1.8×10^5 fold (0.0027 μM) compared to inhibitor B.[35]

Although QuinolineCnSH could not be used for the detection of MBLs by fluorescence, QuinolineCnSH are potent inhibitors for both IMP-1 and VIM-2.

For both PhenylCnSH and QuinolineCnSH, the inhibitory effect is maximum for n=4 for IMP-1 and VIM-2 and least for n=1 for IMP-1. But the effect of variation in the number of methylene units in the linker, n, is different between IMP-1 and VIM-2. The thiol group acts as a coordinating ligand

of one of the two Zn(II) ions or both as a bridging ligand and provides strong driving force for binding with the active center. However, for being a good or relevant inhibitor, candidate compounds should be involved in specific interactions around the environment of the active site. The phenyl group in PhenylC*n*SH and the quinoline group in QuinolineC*n*SH are intended to interact with the hydrophobic region of the enzymes. The dependency of the inhibitory effect on the number of the methylene (*n*) reflects the difference in the geometry of MBL: IMP-1 has a narrower or tighter hydrophobic pocket than VIM-2.

Acknowledgments This study was partially supported by the Research Foundation for Kumamoto Techno Association, Sagawa Science and Technology promotion Foundation to Yamaguchi, a Regional Science Promotion Program of Japan Science and Technology Agency to Kurosaki, Lions Clubs International district 337-D to Jin, and H15-Shinkou-9 from the Ministry of Health, Labor and Welfare of Japan to Goto.

REFERENCES

1) Page M. I., Laws A. P., *Chem. Commun.*, **1998**, 1609—1617 (1998).
2) Page M. I., *Curr. Pharm. Des.*, **5**, 895—913 (1999).
3) Cricco J. A., Vila A. J., *Curr. Pharm. Des.*, **5**, 915—927 (1999).
4) Ambler R. P., *Phil. Trans. R. Soc. Lon.*, **B289**, 321—331 (1980).
5) Galleni M., Lamotte-Brasseur J., Rossolini G. M., Spencer J., Dideberg O., Frère J.-M., *Antimicrob. Agents Chemother.*, **45**, 660—663 (2001).
6) Hussain M., Carlino A., Madonnan M. J., Lampen J. O., *J. Bacteriol.*, **164**, 223—229 (1985).
7) Rasmussen B. A., Gluzman Y., Tally F. P., *Antimicrob. Agents Chemother.*, **34**, 1590—1592 (1990).
8) Arakawa Y., Murakami M., Suzuki K., Ito H., Wacharotayankun R., Ohsuka S., Kato .N., Ohta M., *Antimicrob. Agents Chemother.*, **39**, 1612—1615 (1995).
9) Poirel L., Naas T., Nicolas D., Collet L., Bellais S., Cavallo J.-D., Nordmann P., *Antimicrob. Agents Chemother.*, **44**, 891—897 (2000).
10) Zervosen A., Valladares M. H., Devreese B., Prosperi-Meys C., Adolph H.-W., Mercuri P. S., Vanhove M., Amicosante G., van Beeumen J., Frère J.-M., Galleni M., *Eur. J. Biochem.*, **268**, 3840—3850 (2001).
11) Walsh T. R., Hall L., Assinder S. J., Nichols W. W., Cartwright S. J., MacGowan A. P., Bennett P. M., *Biochim. Biophys. Acta*, **1218**, 199—201 (1994).
12) Concha N. O., Janson C. A., Rowling P., Pearson S., Cheever C. A., Clarke B. P., Lewis C., Galleni M., Frère J.-M., Payne D. J., Bateson J. H., Abdel-Meguid S. S., *Biochemistry*, **39**, 4288—4298 (2000).
13) Concha N. O., Rasmussen B. A., Bush K., Herzberg O., *Structure*, **4**, 823—836 (1996).
14) Shibata N., Doi Y., Yamane K., Yagi T., Kurokawa H., Shibayama K., Kato H., Kai K., Arakawa Y., *J. Clin. Microbiol.*, **41**, 5407—5413 (2003).
15) Walter M. W., Felici A., Galleni M., Soto R. P., Adlington R. M., Baldwin J. E., Frère J.-M., Gololobov M., Schofield C. J., *Bioorg. Med. Chem. Lett.*, **6**, 2455—2458 (1996).
16) Walter M. W.,Valladares M. H., Adlington R. M., Amicosante G., Baldwin J. E., Frère J.-M., Galleni M., Rossolini G. M., Schofield C. J., *Bioorg. Chem.*, **27**, 35—40 (1999).
17) Goto M., Takahashi T., Yamashita F., Koreeda A., Mori H., Ohta M., Arakawa Y., *Biol. Pharm. Bull.*, **20**, 1136—1140 (1997).
18) Bounaga S., Laws A. P., Galleni M., Page M. I., *Biochem. J.*, **331**, 703—711 (1998).
19) Fitzgerald P. M. D., Wu J. K., Toney J. H., *Biochemistry*, **37**, 6791—6800 (1998).
20) Scrofani S. D. B., Chung J., Huntley J. J. A., Benkovic S. J., Wright P. E., Dyson H. J., *Biochemistry*, **38**, 14507—14514 (1999).
21) Greenlee M. L., Laub J. B., Balkovec J. M., Hammond M. L., Hammond G. G., Pompliano D. L., Epstein-Toney J. H., *Bioorg. Med. Chem. Lett.*, **9**, 2549—2554 (1999).
22) Arakawa Y., Shibata N., Shibayama K., Kurokawa H., Yagi T., Fujiwara H., Goto M., *J. Clin. Microbiol.*, **38**, 40—43 (2000).
23) Mollard C., Moali C., Papamicael C., Damblon C., Vessilier S., Amicosante G., Schofield C. J., Galleni M., Frère J.-M., Roberts G. C. K., *J. Biol. Chem.*, **276**, 45015—45023 (2001).
24) Siemann S., Clarke A. J., Viswanatha T., Dmitrienko G. I., *Biochemistry*, **42**, 1673—1683 (2003).
25) Kurosaki H., Yasuzawa H., Yamaguchi Y., Jin W., Arakawa Y., Goto M., *Org. Biomol. Chem.*, **1**, 17—20 (2003).
26) Payne D. J., Bateson J. H., Gasson B. C., Khushi T., Proctor D., Pearson S. C., Reid R., *FEMS Microbiol. Lett.*, **157**, 171—175 (1997).
27) Payne D. J., Bateson J. H., Gasson B. C., Proctor D., Khushi T., Farmer T. H., Tolson D. A., Bell D., Skett P. W., Marshall A. C., Reid R., Ghosez L., Combret Y., Marchand-Brynaert J., *Antimicrob. Agents Chemother.*, **41**, 135—140 (1997).
28) Hammond G. G., Huber J. L., Greenlee M. L., Laub J. B., Young K., Silver L. L., Balkovec J. M., Pryor K. D., Wu J. K., Leiting B., Pompliano D. L., Toney J. H., *FEMS Microbiol. Lett.*, **459**, 289—296 (1999).
29) Payne D. J., Du W., Bateson J. H., *Exp. Opin. Invest. Drugs*, **9**, 247—261 (2000).
30) Bounaga S., Galleni M., Laws A. P., Page M. I., *Bioorg. Med. Chem.*, **9**, 503—510 (2001).
31) Toney J. H., Fitzgerald P. M. D., Grover-Sharma N., Olson, S. H., May W. J., Sundelof J. G., Vanderwall D. E., Cleary K. A., Grant S. K., Wu J. K., Kozarich J. W., Pompliano D. L., Hammond G. G., *Chem. Biol.*, **5**, 185—196 (1998).
32) Toney J. H., Cleary K. A., Hammond G. G., Yuan X., May W. J., Hutchins S. M., Ashton W. T., Vanderwall D. E., *Bioorg. Med. Chem. Lett.*, **9**, 2741—2746 (1999).
33) Nagano R., Adachi Y., Imamura H., Yamada K., Hashizume T., Morishima H., *Antimicrob. Agents Chemother.*, **43**, 2497—2503 (1999).
34) Nagano R., Adachi Y., Hashizume T., Morishima H., *J. Antimicrob. Chemother.*, **45**, 271—276 (2000).
35) Toney J. H., Hammond G. G., Fitzgerald P. M. D., Sharma N., Balkovec J. M., Rouen G. P., Olson S. H., Hammond M. L., Greenlee M. L., Gao Y.-D., *J. Biol. Chem.*, **276**, 31913—31918 (2001).
36) Payne D. J., Hueso-Rodríguez J. A., Boyd H., Concha N. O., Janson C. A., Gilpin M., Bateson J. H., Cheever C., Niconovich N. L., Pearson S., Rittenhouse S., Tew D., Díez E., Pérez P., de la Fuente J., Rees M., Rivera-Sagredo A., *Antimicrob. Agents Chemother.*, **46**, 1880—1886 (2002).
37) Siemann S., Evanoff D. P., Marrone L., Clarke A. J., Viswanatha T., Dmitrienko G. I., *Antimicrob. Agents Chemother.*, **46**, 2450—2457 (2002).
38) Quiroga M. I., Franceschini N., Rossolini G. M., Gutkind G., Bonfiglio G., Franchino L., Amicosante G., *Chemotherapy*, **46**, 177—183 (2000).
39) Carfi A., Duée E., Paul-Soto R., Galleni M., Frère J.-M., Dideberg O., *Acta Cryst.*, **D54**, 47—57 (1998).
40) García-Sáez I., Hopkins J., Papamicael C., Franceschini N., Amicosante G., Rossolini G. M., Galleni M., Frère J.-M., Dideberg O., *J. Biol. Chem.*, **278**, 23863—23873 (2003).
41) García-Saez I., Mercuri P. S., Papamicael C., Kahn R., Frère J.-M., Galleni M., Rossolini G. M., Dideberg O., *J. Mol. Biol.*, **325**, 651—660 (2003).
42) Osano E., Arakawa Y., Wacharotayankun R., Ohta M., Horii T., Ito H., Yoshimura F., Kato N., *Antimicrob. Agents Chemother.*, **38**, 71—78 (1994).
43) Yamaguchi Y., Kuroki T., Yasuzawa H., Jin W., Higashi T., Kawanami A., Taki T., Yamagata Y., Arakawa Y., Goto M., Manuscript in preparation.
44) Goto M., Yasuzawa H., Higashi T., Yamaguchi Y., Kawanami A., Mifune S., Mori H., Nakayama H., Harada K., Arakawa Y., *Biol. Pharm. Bull.*, **26**, 589—594 (2003).
45) Park J. D., Kim D. H., *J. Med. Chem.*, **45**, 911—918 (2002).

ELSEVIER

FEMS Microbiology Letters 243 (2005) 125–131

FEMS MICROBIOLOGY Letters

www.fems-microbiology.org

Measurement of *Pseudomonas aeruginosa* multidrug efflux pumps by quantitative real-time polymerase chain reaction

Kazuhiko Yoneda [a], Hiroki Chikumi [a,*], Takeshi Murata [b], Naomasa Gotoh [b], Hiroyuki Yamamoto [a], Hiromitsu Fujiwara [c], Takeshi Nishino [b], Eiji Shimizu [a]

[a] *Division of Medical Oncology and Molecular Respirology, Department of Multidisciplinary Internal Medicine, Faculty of Medicine, Tottori University, 36-1 Nishi-machi, Yonago-shi, Tottori-ken 683-0805, Japan*

[b] *Department of Microbiology, Kyoto Pharmaceutical University, Yamashina, Kyoto 607-8414, Japan*

[c] *Department of Clinical Laboratory, Tottori University Hospital, 36-1 Nishi-machi, Yonago-shi, Tottori-ken 683-0805, Japan*

Received 21 October 2004; received in revised form 26 November 2004; accepted 29 November 2004

First published online 8 December 2004

Edited by A.M. George

Abstract

Multidrug efflux pumps contribute to multiple antibiotic resistance in *Pseudomonas aeruginosa*. Pump expression usually has been quantified by Western blotting. Quantitative real-time polymerase chain reaction has been developed to measure mRNA expression for genes of interest. Whether this method correlates with pump protein quantities is unclear. We devised a real-time PCR for mRNA expression of MexAB-OprM and MexXY-OprM multidrug efflux pumps. In laboratory strains differing in MexB and MexY expression and in several clinical isolates, protein and mRNA expression correlated well. Quantitative real-time PCR should be a useful alternative in quantitating expression of multidrug efflux pumps by *P. aeruginosa* isolates in clinical laboratories.

Keywords: *Pseudomonas aeruginosa*; Multidrug efflux pumps; Real-time polymerase chain reaction; Western blotting

1. Introduction

Pseudomonas aeruginosa is a clinically important pathogen showing greater intrinsic resistance than most other Gram-negative bacteria to a number of antimicrobial agents. This intrinsic resistance problem is compounded by increasingly frequent development of acquired resistance to agents that ordinarily show potent activity against this organism [1,2]. Thus *P. aeruginosa*, a major opportunistic pathogen, is becoming increasingly difficult to eradicate.

Several mechanisms are known by which this microorganism escapes the toxic effects of antimicrobial agents. These include production of inactivating enzymes, mutations of target enzymes, and multidrug efflux pumps [3–6]. The pumps, especially the resistance-nodulation-division (RND) family, have received particular recent attention because they can extrude multiple structurally unrelated compounds, and thus are involved in multidrug resistance [3,4,7]. To date, at least seven RND family drug efflux pumps are known to exist in *P. aeruginosa* cells. Among them, MexAB-OprM, which is expressed constitutively in wild-type strains, contributes to the intrinsic resistance of *P. aeruginosa* to most β-lactams and many other structurally unrelated antimicrobial agents [2,8,9]. MexXY-OprM also is involved in the intrinsic resistance of *P. aeruginosa* to several agents,

* Corresponding author. Tel.: +81 859 34 8105; fax: +81 859 34 8098.

E-mail address: chikumi@grape.med.tottori-u.ac.jp (H. Chikumi).

0378-1097/$22.00
doi:10.1016/j.femsle.2004.11.048

such as fourth-generation cephems, tetracyclines, erythromycin, and gentamicin [10,11]. Since expression of MexCD-OprJ and MexEF-OprN is strictly suppressed by the respective regulator genes in wild-type *P. aeruginosa* cells, neither of these efflux pumps are involved in intrinsic antibiotic resistance; they contribute only to acquired resistance [12,13].

An important part of investigating resistance mechanisms involving these efflux pumps in *P. aeruginosa* is determination of pump expression levels in laboratory strains or in clinical isolates. Conventionally, this has been done by Western blotting using monoclonal or polyclonal antibodies [1,2,9,14]. However, this method is complex and time-consuming, and the antibodies are not commercially available. A recently, developed new technique, quantitative real-time polymerase chain reaction (PCR), can measure mRNA expression for genes of interest. This method has proven highly accurate and reproducible in quantitating gene expression [15], and can quantify a given mRNA within a very large range of amounts [16]. However, the practicality of using this method to quantify gene expression of *P. aeruginosa* efflux pumps, as well as correlations of mRNA amounts with pump protein amounts, are uncertain. We set out to devise a real-time PCR as a sensitive, easily performed quantitative method for determining expression of two efflux pumps, MexAB-OprM and MexXY-OprM, that contribute to both intrinsic and acquired resistance. We considered this procedure as a possible alternative to quantification of pump proteins by Western blotting.

2. Materials and methods

2.1. Bacterial strains, media and growth conditions

The strains used in this study are shown in Table 1 [1,17,18]. *P. aeruginosa* clinical isolates were randomly selected from our collection at Tottori university hospital and Kyoto pharmaceutical university. Bacterial cells were grown in Luria–Bertani broth (LB) (Wako Pure Chemical Industries, Osaka, Japan). All bacterial cultures in LB were incubated at 37 °C with shaking (140 rpm) for 12.5 h.

2.2. Isolation of total membranes, SDS–PAGE, and immunoblot analysis

Cells grown in LB were harvested by centrifugation and total membranes were prepared as described previously [17]. Sodium dodecyl sulfate–polyacrylamide gel electrophoresis and electrophoretic transfer was performed as described previously [17]. The fractionated proteins were subjected to immunoblot analysis using anti-MexB rabbit-peptid antisera [17] or anti-MexY rabbit polyclonal antibody [32] as the primary antibodies and horseradish peroxidase-linked appropriate secondary antibodies (Pharmacia). The binding antibodies were detected using ECL plus Western blotting detection reagents (Amersham Pharmacia Biotech) according to the manufacture's instructions.

2.3. Cloning in plasmids and quantification of number of copies of the plasmids

Plasmids containing amplified sequences of PAO1 strain were constructed with the pGEM-T Easy Vector Systems (Promega, Tokyo, Japan) according to the manufacture's instructions. Briefly, the fragments of *mexB*, *mexY* and *rpsL* genes, 244, 246 and 241 bp, respectively, were amplified by conventional PCR with the primers listed in Table 2. The fragments were cloned into pGEM-T Easy Vector. DH5α *Escherichia coli* were transformed with these constructions, and after expansion in culture, the plasmids were purified by the Minipreps DNA Purification System (Promega). Gene

Table 1
Pseudomonas aeruginosa strains used in this study

Strain	Description	Source or reference
PAO1	Prototroph	
OCR1	MexAB-OprM-overproducing *nalB* mutant of PAO1	[7]
KG2212	Δ*mexR :: res*-Ω of PAO1	[17]
KG2239	Δ*mexR-mexA-mexB-oprM* of PAO1	[17]
KG5005	MexXY-overproducing, *nalB* Δ*mexAB* of PAO1	[18]
KG4545	*mexZ*::Ω Sm of PAO1	This study[a]
T-001	Clinical isolates	Kyoto Pharmaceutical University
T-002	Clinical isolates	Kyoto Pharmaceutical University
T-003	Clinical isolates	Tottori University
T-004	Clinical isolates	Tottori University
T-005	Clinical isolates	Tottori University
T-006	Clinical isolates	Tottori University
T-007	Clinical isolates	Tottori University
T-008	Clinical isolates	Tottori University
T-009	Clinical isolates	Tottori University

[a] KG4545 was constructed by insertion of Ω Sm cassette into the *mexZ* gene of PAO1 using allele exchange technique.

Table 2
Primers used in this study

Gene	Amplicon size (bp)	Sequences of primers
mexB	244	Forward: GTGTTCGGCTCGCAGTACTC Reverse: AACCGTCGGGATTGACCTTG
mexY	246	Forward: CCGCTACAACGGCTATCCCT Reverse: AGCGGGATCGACCAGCTTTC
rpsL	241	Forward: GCAACTATCAACCAGCTGGTG Forward: GCAACTATCAACCAGCTGGTG

quantification was performed with the BECKMAN DU-64 Spectrophotometer (Beckman Instruments, CA, USA) at a wavelength of 260 nm, and the number of copies was calculated. These plasmids were used as external standards. For each batch, serial plasmid dilutions were amplified; this allowed the construction of a standard curve and the quantification of mRNA in samples.

2.4. RNA extraction and cDNA synthesis

Total RNA was extracted from the 250 μl of cultured medium using QIAGEN RNeasy Mini Kit (Qiagen, Tokyo, Japan), and residual DNA was removed by adding DNase I using QIAGEN RNase-Free DNase Set (Qiagen) according to the manufacture's instructions. RNA was finally dissolved in 50 μl of RNase-free water. For cDNA synthesis, each 20 μl reaction contained 1 μg of total RNA, 10 μg of random hexamer, 1 × first strand buffer (50 mM Tris–HCl (pH 8.3), 75 mM KCl, 3 mM $MgCl_2$; Invitrogen, Tokyo, Japan), 0.5 mM dNTP, 10 U of RNase inhibitor (Invitrogen), and 200 U of Super Script II (Invitrogen). cDNA synthesis was performed in a TaKaRa PCR Thermal Cycler (Takara, Kyoto, Japan) according to the following procedure: after an annealing step for 10 min at 70 °C, reverse transcription was carried out for 50 min at 42 °C, followed by reverse transcriptase inactivation for 10 min at 95 °C.

2.5. Quantitative real-time PCR

The LightCycler (Roche, Tokyo, Japan) was used for all quantitative PCRs. All PCR amplification reactions were performed in a 10 μl volume containing a 3 mM concentration of $MgCl_2$, a 1 μM concentration of forward primers, a 1 μM concentration of reverse primers, 1 × FastStart DNA Master SYBR Green I (Roche), and 1 μl of diluted cDNA (1:10). The cycling parameters used were as follows: one denaturation cycle for 600 s at 95 °C and 45 amplification cycles (temperature transition rate of 20 $°Cs^{-1}$) for 15 s at 95 °C, annealing for 5 s at 55 °C, extension for 10 s at 72 °C. Fluorescence readings were taken after each cycle following the extension step. This was followed by melting curve analysis of 65–99 °C (temperature transition rate of 0.1 $°Cs^{-1}$) with continuous fluorescence readings. For each gene being measured, a sequence-specific standard curve was generated using 10-fold serial dilutions of plasmid DNA containing the sequence of interest and using the appropriate primers. The LightCycler software generated a standard curve from the standards and determined the gene copy number in each test sample. The ratios of gene expression between the target genes (*mexB*, *mexY*) and internal standard (*rpsL*) were expressed relative to those of PAO1 or KG4545, which is set at 1.00.

3. Results

3.1. Design of a real-time PCR assay for quantitative analysis of multidrug efflux pump

MexAB-OprM is considered the most important multidrug efflux pump in *P. aeruginosa*, being involved in broad resistance to cephems, penicillins, monobactams and carbapenems. We therefore first developed a quantitative real-time PCR assay targeted to *mexB* gene expression. Primer sequences were chosen from a region of the *mexB* gene that was preserved among the bacterial strains used in this study, according to DNA sequencing. In addition, an extensive search of several databases, including the EMBL and GenBank databases, indicated that no primer shared significant homology with other known nucleotides sequenced. To determine the copy number of *mexB* gene in sample, a standard curve was established with a control plasmid, pGEM-T/MexB, that contained the target *mexB* partial sequences. The control plasmid was diluted 10-fold with water in a serial manners, from 48 to 4.8×10^7 copies/μl, and each sample was submitted to the *mexB* real-time PCR (Fig. 1(a)). The threshold cycle number, which corresponds to the PCR cycle number at which the fluorescence signal exceeded the detection threshold, was plotted against each of logarithmically increasing standard DNA concentrations. As shown in Fig. 1(b), a linear relationship was obtained over on at least 7-log range of cDNA concentrations.

As MexXY-OprM is the other efflux pump system that contributes to intrinsic and acquired resistance to fourth-generation cephems and aminoglycoside derivative antibiotics, we similarly established a quantitative real-time PCR assay targeted to *mexY* gene expression. The range of quantification was from 88 to 8.8×10^7 copies/μl of pGEM-T/MexY construct (data not shown).

To compensate for varying numbers of cells in samples and efficiency of the reverse transcription reaction, we developed a quantitative real-time PCR reaction for *rpsL*, a constitutively expressed 30S rRNA gene,

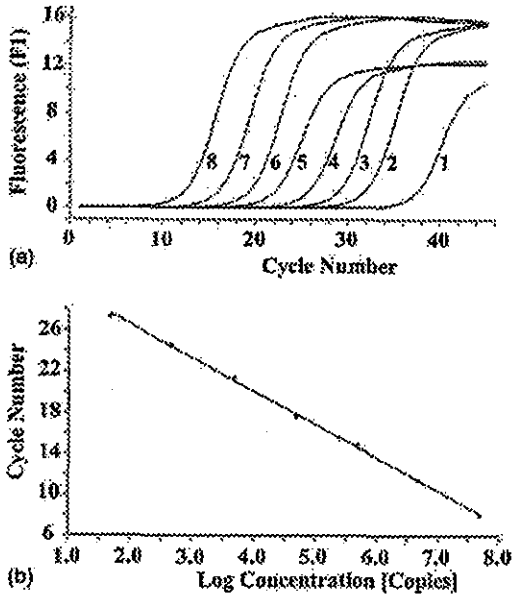

Fig. 1. Amplification profiles (a) and standard curves (b) for Light-Cycler PCR with SYBR Green I. (a) Performance of real-time PCR on a panel of control samples with predetermined numbers of copies of *P. aeruginosa* DNA. The plot shows the relationship of the fluorescent signal to cycle number in a panel of quantified copies of a plasmid containing the *mexB* fragment of a *P. aeruginosa* isolate. Samples: (1), water; (2), 48 copies/μl; (3), 480 copies/μl; (4), 4800 copies/μl; (5), 48,000 copies/μl; (6), 480,000 copies/μl; (7), 4,800,000 copies/μl; (8), 48,000,000 copies/μl. (b) Standard curve for real-time PCR. The threshold cycle number was plotted against each of the logarithmically increasing standard DNA concentrations for calibration.

for use as an internal standard [19]. The sequences of primers were based on previous the report which used them for conventional RT-PCR [20]. Quantitation proved to be linear over a wide logarithmical range, from 57 to 5.7×10^7 copies/l of pGEM-T/RpsL construct (data not shown).

3.2. Correlation between protein and mRNA expression of multidrug efflux pump in laboratory strains

We next used the real-time PCR assay to examine the correlation between protein and mRNA expression of MexB. For this purpose we used four laboratory strains, PAO1, OCR1, KG2212, and KG2239, that had been developed to express MexB to different degrees (Table 1). First we performed Western analysis to quantify protein expression of MexB in these bacterial strains (Fig. 2(a)). Densitometry of the MexB bands respectively showed protein expression in OCR1 and in KG2212 to be 2.9 and 1.3 times greater than in the control strain (PAO1), while no MexB band could be detected in KG2239 (Fig. 2(a)). Up- and down-regulation of MexB was investigated further by real-time PCR after culture under the same conditions. Expression of *mexB* mRNA in OCR1 and KG2212 respectively was 4 and 2.4 times greater than in PAO1, while only traces of *mexB* mRNA were found in KG2239 (Fig. 2(b)). Expression patterns of protein and mRNA thus were highly similar to one another in these laboratory strains.

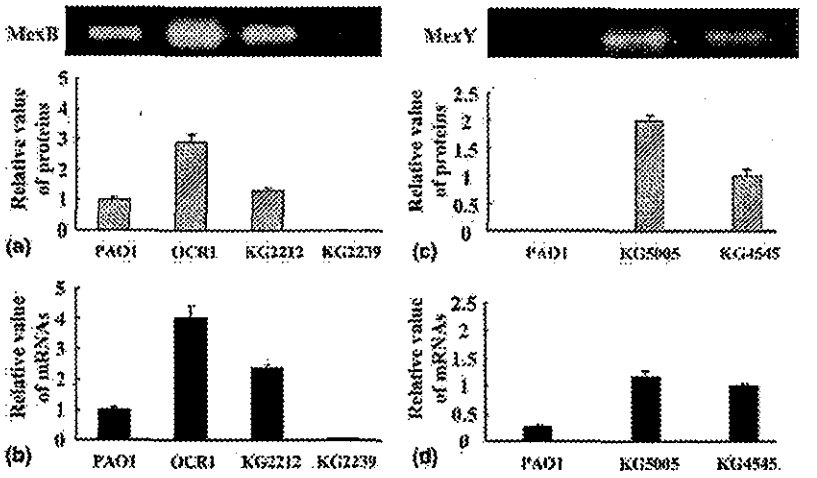

Fig. 2. Correlation between protein and mRNA expression of MexB and MexY in laboratory strains. (a) Western immunoblot analysis using a polyclonal antibody to MexB. Preparation of membranes (5 μg/lane) for immunoblot assay following SDS–PAGE was carried out as described in the Section 2 (upper panel). Band intensity was quantified using the Scion Image program based on the NIH Image for Macintosh program. Data are expressed relative to the quantity of MexB in PAO1. Each bar represents the mean ± SE of the relative intensity in three experiments (lower panel). (b) Quantitation of *mexB* gene expression by real-time PCR. Data are expressed relative to the quantity of *mexB* mRNA in PAO1. Each bar represents the mean ± SE of the relative intensity in three experiments. (c) Western immunoblot analysis using a polyclonal antibody to MexY. Preparation of membranes (5 μg/lane) for immunoblot assay following SDS–PAGE was carried out as described in Section 2 (upper panel). Band intensity was quantified using the Scion Image program based on the NIH Image for Macintosh program. Data are expressed relative to the quantity of MexY in KG4545. Each bar represents the mean ± SE of the relative intensity in three experiments (lower panel). (d) Quantitation of *mexY* gene expression by real-time PCR. Data are expressed relative to the quantity of *mexB* mRNA in KG4545. Each bar represents the mean ± SE of the relative intensity in three experiments.

Next we examined the correlation between protein and mRNA expression of MexY in three laboratory strains, PAO1, KG5005, and KG4545 (Table 1). Western analysis detected bands at 113 kDa representing the MexY protein in KG5005 and KG4545, while no band was seen in PAO1 (Fig. 2(c)). Quantification of the MexY bands showed high degrees of protein expression in KG5005 and KG4545, with expression of KG5005 being twice that of KG4545 (Fig. 2(c)). When expression of *mexY* was examined further by real-time PCR after culture under the same conditions, mRNA expression of *mexY* in KG5005 was 1.2 times that in KG4545, while expression in PAO1 was only 26% of that in KG4545 (Fig. 2(d)). These results were consistent with those of Western blotting.

3.3. Correlation between protein and mRNA expression of multidrug efflux pump in clinical isolates

Since laboratory strains chosen to vary in pump expression showed good correlations between protein and mRNA expression of both MexB and MexY, we next examined the relationship between protein and mRNA expression of MexB in randomly selected clinical isolates (T001 to T009; Table 1). As shown in Fig. 3(a), isolates T001, T002, T003, and T005 showed 1.6–2.3 times greater expression of MexB protein than did PAO1. On the other hand, T004 and T006 to T009, showed 50–100% lower expression than that in PAO1. Corresponding to this protein expression, mRNA expression measured by real-time PCR was higher than in PAO1 in T001, T002, and T003, but lower in T004 and T006 to T009 (Fig. 3(a)). The only exception was T005, which expressed 2.3 times as much protein as PAO1, but only slightly more mRNA.

Next, the same clinical isolates were examined concerning the relationship between protein and mRNA expression of MexY. By Western blotting, in T002 to T006, expression of MexY protein was equal to or greater than that in KG4545, while T001, T007, T008, and T009, like PAO1, did not express detectable MexY protein. In real-time PCR, T002 to T006 expressed more

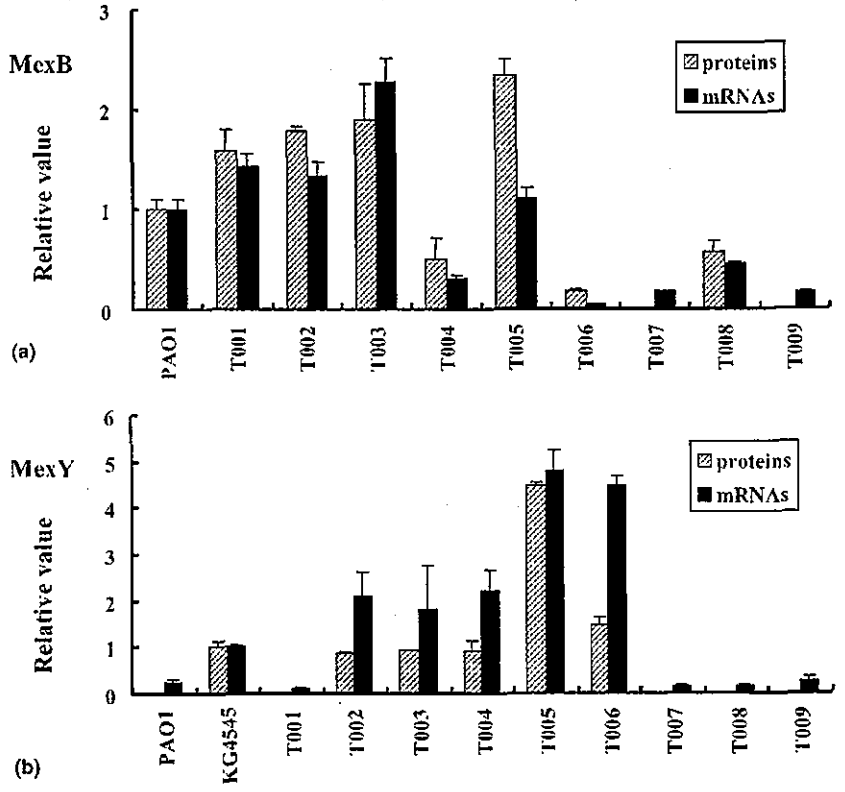

Fig. 3. Correlation between protein and mRNA expression of MexB and MexY in clinical isolates. (a) Hatched bars represent Western immunoblot analysis with a polyclonal antibody to MexB in clinical isolates. Band intensity was quantified using the Scion Image program based on the NIH Image for Macintosh program. Data are expressed relative to the quantity of MexB in PAO1. Each bar represents the mean ± SE of the relative intensity in three experiments. Solid bars represent quantitation of *mexB* gene expression by real-time PCR. Data are expressed relative to the quantity of *mexB* mRNA in PAO1. Each bar represents the mean ± SE of the relative intensity in three experiments. (b) Hatched bars represent Western immunoblot analysis with a polyclonal antibody to MexY in clinical isolates. Band intensity was quantified using the Scion Image program based on the NIH Image for Macintosh program. Data are expressed relative to the quantity of MexY in KG4545. Each bar represents the mean ± SE of the relative intensity in three experiments. Solid bars represent quantitation of *mexY* gene expression by real-time PCR. Data are expressed relative to the quantity of *mexY* mRNA in KG4545. Each bar represents the mean ± SE of the relative intensity in three experiments.

mexY mRNA than KG4545, while T001, T007, T008, and T009 as well as PAO1 expressed only very small amounts of *mexY* mRNA (Fig. 3(b)). Although amounts of protein were relatively small considering those of mRNA in T006, expression patterns of both mRNA and protein levels were quite similar in all other clinical strains. These data showed a general trend of increased protein resulting from increased mRNA.

4. Discussion

In this study we developed a quantitative real-time PCR assay to assess two multidrug efflux pumps in *P. aeruginosa*, MexB and MexY, and examined the relationship between mRNA expression measured by this real-time PCR and protein expression measured by Western blotting. Results obtained with our method, involving RNA isolation, cDNA synthesis, and quantitative real-time PCR, were highly reproducible and permitted precise quantification of minute or substantial amounts of *mexB* or *mexY* mRNA transcripts. Real-time PCR assay allowing quantification of efflux pump gene transcripts relative to those of the 30S rRNA gene, *rpsL*, showed good correlation with MexB and MexY protein expression in laboratory and clinical strains. This real-time PCR would appear to be a useful alternative method for assessing the multidrug efflux pumps MexB and MexY in *P. aeruginosa*.

Of the several techniques developed to estimate protein or mRNA expression, Western blotting is considered the "gold standard" for quantifying expression of multidrug efflux pumps in *P. aeruginosa*. Since this method is time-consuming and requires specific antibodies not commercially available, it has not been widely implemented in clinical laboratories. Real-time PCR has several practical advantages over Western analysis. First, real-time PCR has great sensitivity and a wide effective range. Even though the efflux pump proteins were not detectable in several of our strains, small amounts of corresponding mRNA could be detected and measured in all strains. Secondly, real-time PCR has high throughput and is less labor-intensive than Western analysis; it is a closed-tube system that does not require post-PCR handling. In our experience, total time for specimen processing and analysis is 3–4 h. Third, our application of real-time PCR has broad accessibility, being easy to perform in any laboratory with real-time PCR equipment as long as specific primers have been prepared. Therefore, real-time PCR is an attractive method for estimating gene expression for efflux pumps in bacteria.

As protein expression dose not always exactly reflect mRNA transcription, in case using mRNA expression profiles to presume the protein expression levels, we first needs to confirm the closeness of quantitative correlation of individual proteins with the corresponding mRNA. For example, while several reports have described good correlations between amounts of specific mRNA and corresponding protein expression [21,22], exhaustive studies of bacteria or fungi have reported no significant general correlation between protein and mRNA abundance [22–24]. As for multidrug efflux pumps in *P. aeruginosa*, the few previous studies estimating mRNA expression of these genes by conventional RT-PCR [25], or very recently by real-time PCR [19,26]. However, these works lacked the validation of a correlation between amounts of protein and mRNA expression. We therefore specifically examined this correlation, finding it to be significant for MexB and MexY in *P. aeruginosa*. Our results suggest that quantitative analysis of mRNA by real-time PCR might be a useful indicator of corresponding MexB and MexY protein quantities in lieu of Western blotting.

Although mRNA expression correlated well with protein expression levels in laboratory strains, some clinical isolates showed subtle discrepancies between protein and mRNA expression. Many molecular mechanisms causing these discrepancies have been reported to date. Such mechanisms include post-transcriptional control of the protein translation rate [27], the half-lives of specific proteins or mRNAs [28], and the molecular association of the protein products of expressed genes [29]. Clinical isolates have diverse genetic backgrounds, unlike laboratory strains that are isogenic with a reference strain such as PAO1. Heterogeneity in clinical isolates affects above regulatory mechanisms of transcription, translation, and proteolysis, leading to the discrepancies. In our study, all discrepancies shown in T005 or T006 appear likely to involve overall genetic heterogeneity of the strains, and therefore may be inevitable to some degree in clinical isolates.

In conclusion, real-time PCR based on the capillary format of the LightCycler instrument proved to be a simple, rapid, sensitive, and specific way to quantify multidrug efflux pumps in *P. aeruginosa*. Multidrug resistance of *P. aeruginosa* involves on interplay among multiple resistance mechanisms: β-lactamase, the outer membrane barrier, and multidrug efflux pumps [30,31]; optimal treatment will require a practical method for assessing the latter. Clinical laboratories should be able to estimate expression of these pumps by this method, permitting optimal choices involving antimicrobial agents, as well as antibiotics available for use with multidrug efflux pump inhibitors.

Acknowledgements

This research was partially supported by grants for scientific research to N.G. from the Ministry of Education, Culture, Sports, Science and Technology (MEXT)

of Japan and from the Ministry of Health, Labor and Welfare of Japan.

References

[1] Masuda, N. and Ohya, S. (1992) Cross-resistance to meropenem, cephems, and quinolones in *Pseudomonas aeruginosa*. Antimicrob. Agents Chemother. 36, 1847–1851.

[2] Poole, K., Krebes, K., McNally, C. and Neshat, S. (1993) Multiple antibiotic resistance in *Pseudomonas aeruginosa*: evidence for involvement of an efflux operon. J. Bacteriol. 175, 7363–7372.

[3] Nikaido, H. (2000) Crossing the envelope: how cephalosporins reach their targets. Clin. Microbiol. Infect. 6 (Suppl 3), 22–26.

[4] Hancock, R.E. and Brinkman, F.S. (2002) Function of *Pseudomonas* porins in uptake and efflux. Annu. Rev. Microbiol. 56, 17–38.

[5] Drlica, K. and Zhao, X. (1997) DNA gyrase, topoisomerase IV, and the 4-quinolones. Microbiol. Mol. Biol. Rev. 61, 377–392.

[6] Livermore, D.M. (1992) Interplay of impermeability and chromosomal β-lactamase activity in imipenem-resistant *Pseudomonas aeruginosa*. Antimicrob. Agents Chemother. 36, 2046–2048.

[7] Mine, T., Morita, Y., Kataoka, A., Mizushima, T. and Tsuchiya, T. (1999) Expression in *Escherichia coli* of a new multidrug efflux pump, MexXY, from *Pseudomonas aeruginosa*. Antimicrob. Agents Chemother. 43, 415–417.

[8] Gotoh, N., Tsujimoto, H., Poole, K., Yamagishi, J. and Nishino, T. (1995) The outer membrane protein OprM of *Pseudomonas aeruginosa* is encoded by *oprK* of the *mexA-mexB-oprK* multidrug resistance operon. Antimicrob. Agents Chemother. 39, 2567–2569.

[9] Li, X.Z., Nikaido, H. and Poole, K. (1995) Role of MexA-MexB-OprM in antibiotic efflux in *Pseudomonas aeruginosa*. Antimicrob. Agents Chemother. 39, 1948–1953.

[10] Masuda, N., Sakagawa, E., Ohya, S., Gotoh, N., Tsujimoto, H. and Nishino, T. (2000) Contribution of the MexX-MexY-oprM efflux system to intrinsic resistance in *Pseudomonas aeruginosa*. Antimicrob. Agents Chemother. 44, 2242–2246.

[11] Masuda, N., Sakagawa, E., Ohya, S., Gotoh, N., Tsujimoto, H. and Nishino, T. (2000) Substrate specificities of MexAB-OprM, MexCD-OprJ, and MexXY-oprM efflux pumps in *Pseudomonas aeruginosa*. Antimicrob. Agents Chemother. 44, 3322–3327.

[12] Kohler, T., Michea-Hamzehpour, M., Henze, U., Gotoh, N., Curty, L.K. and Pechere, J.C. (1997) Characterization of MexE-MexF-OprN, a positively regulated multidrug efflux system of *Pseudomonas aeruginosa*. Mol. Microbiol. 23, 345–354.

[13] Poole, K., Gotoh, N., Tsujimoto, H., Zhao, Q., Wada, A., Yamasaki, T., Neshat, S., Yamagishi, J., Li, X.Z. and Nishino, T. (1996) Overexpression of the *mexC-mexD-oprJ* efflux operon in *nfxB*-type multidrug-resistant strains of *Pseudomonas aeruginosa*. Mol. Microbiol. 21, 713–724.

[14] Srikumar, R., Li, X.Z. and Poole, K. (1997) Inner membrane efflux components are responsible for β-lactam specificity of multidrug efflux pumps in *Pseudomonas aeruginosa*. J. Bacteriol. 179, 7875–7881.

[15] Gibson, U.E., Heid, C.A. and Williams, P.M. (1996) A novel method for real time quantitative RT-PCR. Genome Res. 6, 995–1001.

[16] Heid, C.A., Stevens, J., Livak, K.J. and Williams, P.M. (1996) Real time quantitative PCR. Genome Res. 6, 986–994.

[17] Gotoh, N., Tsujimoto, H., Tsuda, M., Okamoto, K., Nomura, A., Wada, T., Nakahashi, M. and Nishino, T. (1998) Characterization of the MexC-MexD-OprJ multidrug efflux system in Δ *mexA-mexB-oprM* mutants of *Pseudomonas aeruginosa*. Antimicrob. Agents Chemother. 42, 1938–1943.

[18] Murata, T., Gotoh, N. and Nishino, T. (2002) Characterization of outer membrane efflux proteins OpmE, OpmD and OpmB of *Pseudomonas aeruginosa*: molecular cloning and development of specific antisera. FEMS Microbiol. Lett. 217, 57–63.

[19] Hocquet, D., Bertrand, X., Kohler, T., Talon, D. and Plesiat, P. (2003) Genetic and phenotypic variations of a resistant *Pseudomonas aeruginosa* epidemic clone. Antimicrob. Agents Chemother. 47, 1887–1894.

[20] Westbrock-Wadman, S., Sherman, D.R., Hickey, M.J., Coulter, S.N., Zhu, Y.Q., Warrener, P., Nguyen, L.Y., Shawar, R.M., Folger, K.R. and Stover, C.K. (1999) Characterization of a *Pseudomonas aeruginosa* efflux pump contributing to aminoglycoside impermeability. Antimicrob. Agents Chemother. 43, 2975–2983.

[21] Futcher, B., Latter, G.I., Monardo, P., McLaughlin, C.S. and Garrels, J.I. (1999) A sampling of the yeast proteome. Mol. Cell Biol. 19, 7357–7368.

[22] Washburn, M.P., Koller, A., Oshiro, G., Ulaszek, R.R., Plouffe, D., Deciu, C., Winzeler, E. and Yates 3rd, J.R. (2003) Protein pathway and complex clustering of correlated mRNA and protein expression analyses in *Saccharomyces cerevisiae*. Proc. Natl. Acad. Sci. USA 100, 3107–3112.

[23] Griffin, T.J., Gygi, S.P., Ideker, T., Rist, B., Eng, J., Hood, L. and Aebersold, R. (2002) Complementary profiling of gene expression at the transcriptome and proteome levels in *Saccharomyces cerevisiae*. Mol. Cell Proteomics 1, 323–333.

[24] Gygi, S.P., Rochon, Y., Franza, B.R. and Aebersold, R. (1999) Correlation between protein and mRNA abundance in yeast. Mol. Cell Biol. 19, 1720–1730.

[25] Evans, K., Adewoye, L. and Poole, K. (2001) MexR repressor of the *mexAB-oprM* multidrug efflux operon of *Pseudomonas aeruginosa*: identification of MexR binding sites in the *mexA-mexR* intergenic region. J. Bacteriol. 183, 807–812.

[26] Llanes, C., Hocquet, D., Vogne, C., Benali-Baitich, D., Neuwirth, C. and Plesiat, P. (2004) Clinical strains of *Pseudomonas aeruginosa* overproducing MexAB-OprM and MexXY efflux pumps simultaneously. Antimicrob. Agents Chemother. 48, 1797–1802.

[27] Nogueira, T. and Springer, M. (2000) Post-transcriptional control by global regulators of gene expression in bacteria. Curr. Opin. Microbiol. 3, 154–158.

[28] Varshavsky, A. (1996) The N-end rule: functions, mysteries, uses. Proc. Natl. Acad. Sci. USA 93, 12142–12149.

[29] Gerth, U., Kirstein, J., Mostertz, J., Waldminghaus, T., Miethke, M., Kock, H. and Hecker, M. (2004) Fine-tuning in regulation of Clp protein content in *Bacillus subtilis*. J. Bacteriol. 186, 179–191.

[30] Li, X.Z., Zhang, L. and Poole, K. (2000) Interplay between the MexA-MexB-OprM multidrug efflux system and the outer membrane barrier in the multiple antibiotic resistance of *Pseudomonas aeruginosa*. J. Antimicrob. Chemother. 45, 433–436.

[31] Okamoto, K., Gotoh, N. and Nishino, T. (2001) *Pseudomonas aeruginosa* reveals high intrinsic resistance to penem antibiotics: penem resistance mechanisms and their interplay. Antimicrob. Agents Chemother. 45, 1964–1971.

[32] Hocquet, D., Vogne, C., El Garch, F., Vejux, A., Gotoh, N., Lee, A., Lomovskaya, O. and Plesiat, P. (2003) MexXY-OprM efflux pump is necessary for a adaptive resistance of *Pseudomonas aeruginosa* to aminoglycosides. Antimicrob. Agents Chemother. 47, 1371–1375.

JOURNAL OF CLINICAL MICROBIOLOGY, Jan. 2005, p. 458–461
0095-1137/05/$08.00+0 doi:10.1128/JCM.43.1.458–461.2005

Vol. 43, No. 1

Clonal Diversity of Metallo-β-Lactamase-Possessing *Pseudomonas aeruginosa* in Geographically Diverse Regions of Japan

Soichiro Kimura,[1] Jimena Alba,[1] Katsuaki Shiroto,[1] Reiko Sano,[2] Yoshihito Niki,[3] Shigefumi Maesaki,[4] Koji Akizawa,[5] Mitsuo Kaku,[6] Yuji Watanuki,[7] Yoshikazu Ishii,[1]* and Keizo Yamaguchi[1]

Department of Microbiology, Toho University School of Medicine, Tokyo[1]; Nara Medical University, Nara[2]; Kawasaki Medical School, Okayama[3]; Saitama Medical School, Saitama[4]; Hokkaido University Hospital, Sapporo[5]; Tohoku University Graduate School of Medicine, Miyagi[6]; and Kanagawa Cardiovascular and Respiratory Diseases Center, Kanagawa,[7] Japan

Received 24 March 2004/Returned for modification 30 April 2004/Accepted 1 June 2004

The aim of this study was to determine the distribution of metallo-β-lactamase-producing *Pseudomonas aeruginosa* in Japan and to investigate the molecular characteristics of resistance gene cassettes including the gene encoding this enzyme. A total of 594 nonduplicate strains of *P. aeruginosa* isolated from 60 hospitals throughout Japan in 2002 were evaluated. This study indicated that although the prevalence of imipenem-resistant *P. aeruginosa* has not increased compared to that found in previous studies, clonal distribution of the same strain across Japan is evident.

Class A, B, and D β-lactamases, as defined by Ambler et al., can hydrolyze carbapenems (1, 9). In particular, class B β-lactamases, termed metallo-β-lactamases, are an increasingly serious clinical problem because they have a very broad substrate profile that includes penicillins, expanded-spectrum cephalosporins, and carbapenems and excludes only monobactams, such as aztreonam. It has been reported that IMP-1 metallo-β-lactamase-producing *Serratia marcescens* was first isolated in Japan in 1991 (10). Recently, metallo-β-lactamase-producing *Pseudomonas aeruginosa* and *S. marcescens* probably have the highest incidence of isolation in Japan (7).

Most metallo-β-lactamase genes are located on integrons, which are genetic elements containing gene cassettes that can facilitate their spread and mobilize the genes to other integrons or to other sites. The gene cassettes often encode clinically important antibiotic resistance genes, including those encoding β-lactamases such as extended-spectrum β-lactamases and carbapenemases, and also aminoglycoside-modifying enzymes (12).

Little is known about the distribution of the clone(s) that produces metallo-β-lactamases in Japan. Therefore, we conducted a surveillance study covering a wide geographic area with the aim of determining the distribution of metallo-β-lactamase producers in Japan and to investigate the molecular characteristics of the resistance gene cassettes that included the gene encoding a metallo-β-lactamase.

A total of 594 nonduplicate strains of *P. aeruginosa* isolated from 60 hospitals throughout Japan in the year 2002 were evaluated. The susceptibility of *P. aeruginosa* to several antibiotics was measured with the Etest strip, and the strains were stored on Casitone medium (Eiken Chemical Co. Ltd., Tokyo, Japan) (data not shown). After 6 months, the antibiotic susceptibility of these isolates was reassessed by the National Committee for Clinical Laboratory Standards broth microdilution method with cation-adjusted Mueller-Hinton broth (Difco, Detroit, Mich.). The isolates were screened for the presence of metallo-β-lactamase by a double-disk synergy test reported by Arakawa et al. (2). Integron analysis was performed by PCR mapping (5′-conserved segment *int*I to 3′-conserved segment *qacE*Δ*1*) of the typical antibiotic resistance genes and integron with specific primer sets (Table 1). The specificity of the primer sets for bla_{IMP-1}-like and bla_{VIM-2}-like gene was confirmed with positive-control strains producing IMP-1 or VIM-2 metallo-β-lactamase. The specificity of amplicons obtained by specific primer sets (*aacA4*, *aadA1*, *aadA2*, and bla_{OXA-2}) was also partially verified with the automatic sequencer ABI Prism 310 genetic analyzer (Applied Biosystems/Perkin-Elmer Biosystems). PCR with Ex *Taq* polymerase (Takara Bio, Inc., Tokyo, Japan) were carried out by standard methodology (13). pulsed-field gel electrophoresis analysis was performed by a modified method of the standard protocol (6). The restriction enzyme used was SpeI (15). By use of the dendrogram, isolates with a genetic relatedness of >80% were

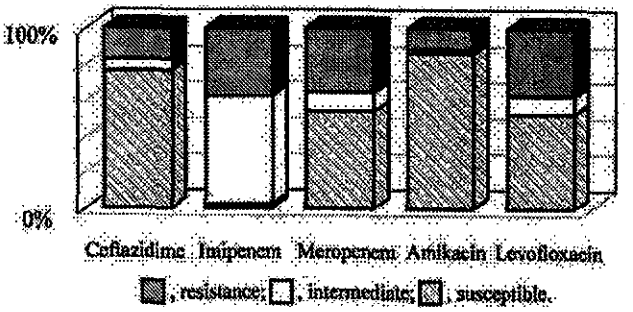

FIG. 1. Antimicrobial susceptibilities of imipenem-nonsusceptible *P. aeruginosa* isolates.

* Corresponding author. Mailing address: Department of Microbiology, Toho University School of Medicine, 5-21-16 Omori-nishi, Ota-ku, Tokyo 1438540, Japan. Phone: 81-3-3762-4151, ext. 2396. Fax: 81-3-5493-5415. address: E-mail: yoishii@med.toho-u.ac.jp.

TABLE 1. Nucleotide sequences of PCR primers used in this study

Gene[a]	Primer sequence (5' to 3')	T_m (°C)	Reference
*int*A(S)	ATC ATC GTC GTA GAG ACG TCG G	67.4	11
*int*B(AS)	GTC AAG GTT CTG GAC CAG TTG C	66.9	11
bla_{IMP-1}(S)	CTA CCG CAG CAG AGT CTT TG	62.7	This study
bla_{IMP-1}(AS)	AAC CAG TTT TGC CTT ACC AT	59.9	This study
bla_{VIM-2}(S)	AAA GTT ATG CCG CAC TCA CC	63.9	This study
bla_{VIM-2}(AS)	TGC AAC TTC ATG TTA TGC CG	64.5	This study
aacA4(S)	GAC CTT GCG ATG CTC TAT GAG TGG CTA AAT	73.0	This study
aacA4(AS)	TTC GCT CGA ATG CCT GGC GTG TT	76.9	This study
aadA1(S)	TGA TCG CCG AAG TAT CGA CTC	66.3	This study
aadA1(AS)	CCT TGG TGA TCT CGC CTT TC	65.8	This study
aadA2(S)	TTC GAA CCA ACT ATC AGA GGT GCT AA	67.4	This study
aadA2(AS)	AAA GCG AAT AAA TTC TTC CAA GTG ATC T	66.4	This study
bla_{OXA-2}(S)	CAA TCC GAA TCT TCG CGA TAC TT	66.9	This study
bla_{OXA-2}(AS)	AAG TAT CGC GAA GAT TCG GAT TG	66.9	This study
qacEΔ1	CTC TCT AGA TTT TAA TGC GGA TG	60.6	This study

[a] (S), sense; (AS), antisense.

considered to represent the same pulsed-field gel electrophoresis type (4).

Eighty-eight (15%) of 594 isolates were not susceptible (MIC ≥ 8 mg/ml) to imipenem. Among 88 isolates, 88 (100%), 21 (24%), 41 (47%), 12 (14%), and 42 (48%) were not susceptible to imipenem, ceftazidime, meropenem, amikacin, and levofloxacin, respectively (Fig. 1). Screening of metallo-β-lactamase producers was carried out for these isolates by the double-disk synergy test. Eleven (1.9%) of 594 isolates were found to produce metallo-β-lactamase. Ten of these isolates were IMP-1-like, and the other was a VIM-2-like metallo-β-lactamase producer.

The type of metallo-β-lactamase gene was also confirmed by PCR. The genetic relatedness of these isolates was also evaluated by pulsed-field gel electrophoresis as described above (Fig. 2, Table 2). Strains TUM1683, TUM1708, TUM1709, TUM1710, and TUM1732 had related electrophoresis chromosomal DNA banding patterns, whereas other strains (TUM1672, TUM1673, TUM1682, TUM1721, TUM1733, and TUM1757) showed different banding patterns. Strain TUM1708, TUM1709, and TUM1710 were isolated from same hospital, suggesting nosocomial spread. Interestingly, although strains TUM1683, TUM1708 (or TUM1709 and TUM1710), and TUM1732 has been isolated in different hospitals, Kawasaki, Saitama, and Nara, respectively, these isolates had related patterns. Since the distance from Okayama to Saitama and from Saitama to Nara is about 800 and 400 km, respectively, the results observed suggested clonal spread of metallo-β-lactamase-producing strains.

Several researchers have reported an incidence of metallo-β-lactamase-producing *P. aeruginosa* of between 0.4 and 1.3% in Japan from 1992 to 2002 (5, 7, 14, 16). In this study, we isolated 1.9% metallo-β-lactamase-producing *P. aeruginosa* strains from geographically diverse regions in Japan. We suggest that the incidence of metallo-β-lactamase-possessing *P. aeruginosa* has not increased during the past decade. However, the same clone of metallo-β-lactamase-carrying *P. aeruginosa* has now spread throughout Japan.

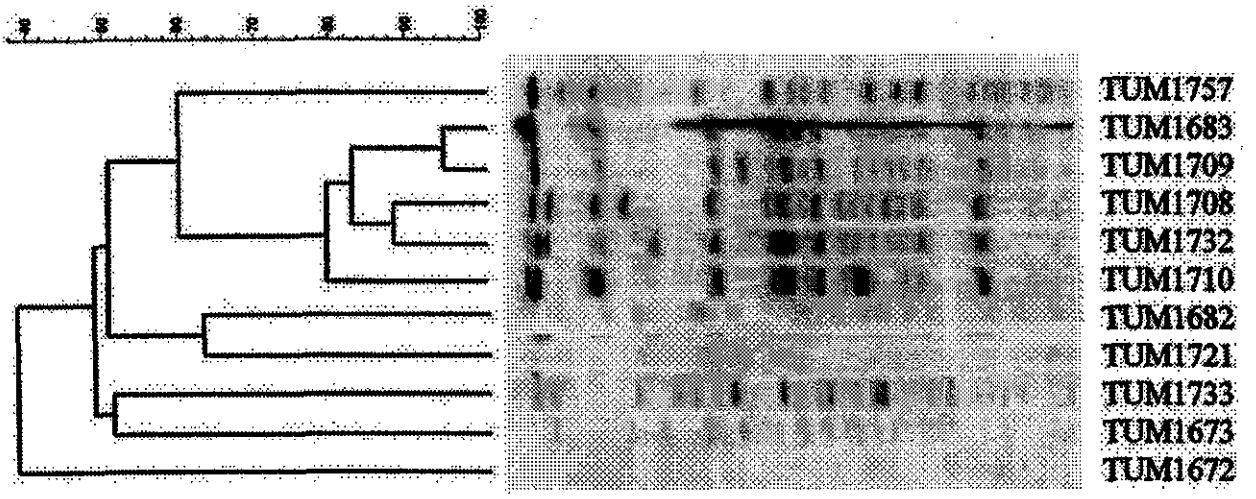

FIG. 2. Pulsed-field gel electrophoresis profiles obtained with SpeI chromosomal digestion of metallo-β-lactamase-carrying *P. aeruginosa*. The second through sixth lanes contained related strains TUM1683, TUM1709, TUM1708, TUM1732, and TUM1710, respectively. Lanes first and seventh to eleventh lanes contained unrelated strains TUM1757, TUM1682, TUM1721, TUM1733, TUM1673, and TUM1672, respectively.